This is the Pre-Published Version.

This material may be downloaded for personal use only. Any other use requires prior permission of the American Society of Civil Engineers. This material may be found at https://doi.org/10.1061/(ASCE)CO.1943-7862.0002113.

An Integrative Evolutionary-based Method for Modeling and Optimizing Budget Assignment of Bridge Maintenance Priorities

Eslam Mohammed Abdelkader*[1,2], Osama Moselhi[3], Mohamed Marzouk[4], and Tarek Zayed[5]

ABSTRACT

Recently, the number of deteriorating bridges has drastically increased. As such, enormous amount of resources are invested yearly to maintain the performance of bridges within acceptable levels. This entails the development of bridge management systems to manage the imbalance between the extensive needs for maintenance, repair and rehabilitation actions, and the limited available funds. In this regard, the present study introduces three-tier platform to model and allocate limited resources in bridge deck replacement projects. The first model involves building a discrete event simulation model to mimic the bridge deck replacement process. The second encompasses structuring an efficient and straightforward surrogate machine learning model for mimicking the computationally expensive discrete event simulation model. In the second phase, a novel hybrid Elman neural network-Invasive weed optimization model is developed for predicting time, cost, greenhouse gases and utilization rates of resource allocation plans using database generated from the previous model. The third constitutes formulation of a multi-objective differential evolution optimization model subject to the utilization rates of the involved resources and their dispersion. Results manifest superiority in cost prediction accuracies; achieving mean absolute percentage error, mean absolute error and root-mean squared error of 4.873%, 78.466 and 39.515, respectively. Additionally, the developed multi-objective optimization model significantly outperformed a set well-performing meta-heuristics;

[1] Ph.D. candidate, Department of Building, Civil, and Environmental Engineering, Concordia University, Montreal, QC, Canada. Corresponding author, E-mail: eslam_ahmed1990@hotmail.com.
[2] Assistant lecturer, Structural Engineering Department, Faculty of Engineering, Cairo University, Egypt.
[3]Professor and Director of the Centre for Innovation in Construction and Infrastructure Engineering and Management (CICIEM), Department of Building, Civil, and Environmental Engineering, Concordia University, Montreal, QC, Canada.
[4] Professor of Construction Engineering and Management, Structural Engineering Department, Faculty of Engineering, Cairo University, Egypt.
[5] Professor, Department of Building and Real Estate, the Hong Kong Polytechnic University, Hung Hom, Hong Kong.

The following publication Abdelkader, E. M., Moselhi, O., Marzouk, M., & Zayed, T. (2021). Integrative Evolutionary-Based Method for Modeling and Optimizing Budget Assignment of Bridge Maintenance Priorities. Journal of Construction Engineering and Management, 147(9), 04021100 is available at https://doi.org/10.1061/(ASCE)CO.1943-7862.0002113.

yielding hypervolume indicator, generational distance, spacing, diversity, spread and coverage of 81.721%, 0.029, 0.1881, 0.5229, 0.9618 and 0.4087, respectively. Results also demonstrate the developed multi-objective optimization model accomplished an improvement in minimization time, cost and greenhouse gases by 71.01%, 27.87% and 39.29%respectively when compared against genetic algorithm. The developed models are automated through hybrid programming of C#.net and Matlab. It is expected that the developed method can enable the practitioners and transportation agencies in establishing timely-efficient, cost-effective and sustainable resource allocation plans while accommodating efficacious utilization of resources

Keywords: Bridge deck replacement; Discrete event simulation; Surrogate machine learning; Elman neural network; Invasive weed optimization; Multi-objective differential evolution optimization

1. INTRODUCTION

Bridges are vital links in transportation networks, and it is crucial to maintain them within acceptable performance limits despite the harsh operating conditions. In the recent years, the number of worldwide deficient bridges has increased (Rojob and El-Hacha, 2018). Owing to the fact there are limited available funds for maintenance, repair and rehabilitation actions. This motivated researchers and decision-makers to pay more attention for the maintenance planning of deteriorating bridges, which is demonstrated in the form of efficient bridge management systems (Tesfamariamet al., 2018). The American Association of State Highway and Transportation Officials (AASHTO) defined Bridge Management System (BMS) as “a system designed to optimize the use of available resources for inspection, maintenance, rehabilitation and replacement of bridges” (AASHTO, 2011). Bridge management systems assist in overcoming the backlog in maintaining the bridge structures, whereas the backlog of maintenance activities can result in the increase of repair costs to the extent that repairing the deteriorating bridges is more expensive than building new ones (Miyamoto et al., 2001).

In Canada, the instantaneous and serious economic and environmental impacts of bridge collapses alongside their high owner and user costs have drawn the public attention towards the importance of bridge management systems (Ali et al., 2019). Bridges experience accelerated aging and extensive deterioration and larger portion of them require urgent rehabilitation or replacement. They consumed approximately 57% of their useful time, whereas their average age is considered as the second highest among the five main assets, namely roads, bridges, water supply systems, wastewater treatment facilities and sewer systems (Statistics Canada, 2009). It was also reported that 26% of the bridges are either in a “Fair”, “Severe” or “Very Severe” condition categories (Felio, 2016).

Bridges in Quebec experienced higher levels of deterioration such that they reached 72% of their useful lifetime, which is regarded as the highest average age among all the provinces of Canada. On the other hand, bridges in Prince Edward Island have the smallest average age, which is 15.6 years. This can be attributed to that about 70% of the bridges in Quebec were built between the 1960s and 1980s (Farzam et al., 2016; Viami International Inc. and the Technology Strategies Group, 2013). The backlog of bridge maintenance, rehabilitation and replacement is estimated to be equal to $10 billion. The continuous increase in the backlog results in a significant deterioration in the condition of the bridge elements (Sennah et al., 2011). As such, expeditious deteriorating condition coupled with increase in public demands for safe, functional and serviceable transportation networks in the light of squeezed maintenance and intervention budgets constitute an escalating challenge for the departments of transportation to optimize the allocation of resources consumed in bridge maintenance activities. In this regard, the primary aim of this research study is to develop an automated integrative evolutionary-based paradigm, which aids decision makers to model and optimize the performance aspects and utilization rates

of resource allocation plans in bridge deck replacement projects based on technical, economic and environmental aspects while ensuring the efficacy in the utilization of resources. This is achieved through the following group of objectives:

1- Develop a discrete event simulation model to emulate the bridge deck replacement process.
2- Build a data-driven surrogate machine learning model to simulate automatically the performance aspects and utilization rates of different resource allocation plans.
3- Formulate a multi-objective optimization model for resource allocation that accommodates the competing objectives of time, cost and greenhouse gas emissions while satisfying utilization requirements.
4- Validate the developed models through a set of performance and statistical comparisons.

2. LITERATURE REVIEW

The literature review encompasses two sections namely, resource-based planning and maintenance allocation.

2.1 Resource-based Panning

Resource-based planning and scheduling is essential for the cost-effective and reliable delivery of construction projects. Several research studies were carried out to analyze and solve the problems pertinent to resource allocation in different types of construction projects. Osman et al. (2017) proposed a simulation-based multi-objective optimization model to schedule repair costs in water network break sites. Results demonstrated that the developed genetic algorithm-based model was able to reduce repair time by 21% with respect to the developed optimization model by the water municipality. Vand Xavier (2017) introduced a resource driven scheduling model that utilized genetic algorithm to optimally allocate resources to repetitive activities of

high rise buildings. The generated schedule encompassed number of days required to complete needed activities, their sequential order and the required material and equipment.

Podolski and Sroka (2019) introduced a cost optimization model for multi-unit construction projects. The optimal work schedule was generated using simulated annealing-based model that aimed at minimizing direct costs, indirect costs, costs of misleading deadlines and costs of work group discontinuities. Tomczak and Jaśkowski (2020) presented a deterministic mathematical model that incorporated the use of mixed integer programming to minimize the downtime days of general contractor's crews in repetitive construction projects. The developed model was able to consider project deadlines, limited budget and limited availability of crews. Limsawasd and Athigakunagorn (2017) proposed a discrete event simulation-based model to manually optimize resource allocation and enhance work productivity in scaffolding work of building projects. Different crew configurations were generated and analyzed according to the total construction time, total construction cost and total awaiting time of workers in an attempt to obtain the optimal resource allocation strategy.

Zou et al. (2018) developed a bi-optimization model that comprised the use of mixed integer programming for the purpose of minimizing total number of crews and maximizing work discontinuity in repetitive projects. The developed model was based on line of balance scheduling to monitor work continuity in highway projects. It also encompassed an additional module to minimize work interruptions while maintaining the pre-defined objective functions. Jaskowski and Biruk (2020) introduced an optimization model for the minimization of idle time of crews while satisfying the contractual project duration in school buildings. In it, mixed binary linear programming was adopted to generate an optimal schedule that included the start and

finishing dates for the different processes of the zones based on the optimum configuration of resources and optimum routing of crews.

The literature lacks studies that dealt with resource-based planning of bridge maintenance projects. Few studies were proposed to optimize resource allocation plans in bridge deck maintenance projects. Zhang et al. (2008) introduced a discrete event simulation model to analyze resource combinations of bridge deck rehabilitation. In this context, sensitivity analysis was conducted to select the optimum resource combination that yielded less unit cost and higher productivity. It was also found that most of the previous studies pertinent to bridge maintenance management focused on project level or network level maintenance budget allocation rather than investigating the optimization of the rehabilitation work at the element level, which is primarily concerned with resource allocation under multiple conflicting objective functions. Several attempts have been conducted to develop multi-objective optimization and prioritization models for the purpose of bridge maintenance management, which provide bridge managers with several optimal plans. They are described in the following lines.

2.2 Maintenance Allocation

2.2.1 Optimization-based models

Bukhsh et al. (2020) developed a multi-year maintenance planning framework for bridges at a network level. They utilized discrete Markov decision process to model the bridge deterioration process, whereas percentage prediction method was applied to calibrate the transition probability matrices. They employed multi-attribute utility theory to sort the bridges by capturing the different defining attributes and decision makers' preferences. Genetic algorithm was applied to find the optimal maintenance plans by accommodating the performance requirements and tight budget constraints. Mao et al. (2020) designed an optimal maintenance

scheduling strategy that was formulated in the form of two levels. The upper level incorporated a multi-objective non-linear programming model, which aimed at minimizing the total traffic delays during the maintenance period and maximizing the total number of bridges to be repaired. The lower level comprised simulating users' route choice using a modified user equilibrium model, whereas simulated annealing algorithm was deployed to solve the optimization model.

Mahdi et al. (2019) developed a decision support system to prioritize the maintenance strategies of concrete bridges using dynamic programming. The evaluation criteria of the bridges depended on some performance indicators which included: structural performance, functional performance and external factors. They highlighted that the developed model can compute the optimal maintenance plan for each bridge within the network while taking the budget constraints within limitations. Wu et al. (2017) designed an optimization model to enable the transportation agencies to allocate the funds of the bridge maintenance based on minimizing the life cycle costs and maximizing the structural performance of the whole lifespan bridge. The 2012 National Bridge Inventory (NBI) of the state of Texas was used as an input to build the optimization model.

Shim and Lee (2017) constructed a multi-objective optimization model with linearly weighted sum method to define the optimum maintenance, repair and rehabilitation (MR&R) activities for a network of bridge decks. The developed optimization model encompassed minimizing the area percentages of structurally deficient decks and minimizing the annual MR&R budget. The beta distribution was used to model the uncertainties of the unit cost of the intervention actions rather than employing deterministic values. Badawy (2017) developed an optimization model to select the optimum MR&R activities for expansion joints. The optimum intervention actions were defined using genetic algorithm based on maximizing the overall condition of the expansion

joints given a certain budget constraint. Additionally, the transition probability matrix was calibrated stepping on minimizing the differences between the predicted condition and the inspected condition.

2.2.2 Multi-criteria decision making-based models

Contreras-Nieto et al. (2019) introduced a geographical information system (GIS)-based multi-criteria decision making model for bridge maintenance prioritization. They established a weighted bridge rating system using analytical hierarchy process by analyzing responses from local bridge experts. The bridge rating system was designed as per weighted average of deck, substructure, superstructure and scour with respect to resiliency, riding comfort, safety and serviceability. They concluded that the developed model could visualize the prioritization of bridges for maintenance, which improves the decision-making process in the departments of transportation. Yossyafra et al. (2019) presented a hybrid multi-criteria decision making model for maintenance prioritization of bridges in West Sumatra Province. They utilized fuzzy analytical hierarchy process to compute the weights of attributes, which were technical condition, age, average daily traffic, economic benefits, road function, budget fund, disaster impact and spatial conditions. Then, a multi-criteria ranking index was calculated using VIKOR method, which mapped the priority order of bridges to be repaired prior to others.

Bukhsh et al. (2019) presented an approach for network level maintenance planning using multi-attribute utility theory. The proposed approach prioritized the bridges by accommodating different attributes which were: improving assets' reliability, minimizing agency cost, minimizing impact on users and maintaining the bridge network safety. They suggested that the proposed approach can improve the decision-making of maintenance planning through modeling performance, economic and social aspects. Markiz and Jrade (2018) presented a fuzzy-based

decision support system integrated with bridge information management system to model the bridge deterioration modeling and to prioritize the maintenance, repair and rehabilitation actions at the conceptual design stage. They applied time-dependent gamma shock model to forecast the bridge deterioration. Furthermore, technique of order preference by similarity to ideal solution (TOPSIS) was deployed to design the maintenance prioritization platform of bridges. They highlighted that the developed model was capable of attaining approximately 10%-15% error in the prediction accuracy of bridge deterioration.

Rashidi et al. (2017) presented a decision support system to rank the remedial actions of steel bridges using analytical hierarchy process. They considered a set of attributes to model the remedial actions such as safety, service life, remediation cost, traffic disruption, environmental impact and heritage significance. They modeled four alternatives of rehabilitation actions which were: splice plates, steel plate strengthening, fiberglass reinforced plastic strengthening and partial member replacement. They concluded that the presented model can enable asset managers to manage the bridges through balanced modeling of multiple attributes. Yoon and Hastak (2017) presented a multi-tiered prioritization method for ranking bridge deck rehabilitation projects as per urgency scale and total prioritization scale. The urgency scale was defined according to the physical condition of the bridge deck while the total prioritization scale was constructed as a result of integration of the normalized values of performance, economic and criticality scales.

Nurdin et al. (2017) developed a multi-criteria decision making model to set a priority scale for bridge maintenance and rehabilitation. Three attributes were introduced to set the maintenance prioritization index, whereas the criteria for condition of damage represented the largest weight followed by the volume traffic and criteria policy. The weights of attributes were computed based on analytical hierarchy process by aggregating the feedback of 27 respondents using

geometric mean. ArcGIS was utilized to visualize the output of the maintenance prioritization model. Amini et al. (2016) proposed a decision-making model to prioritize the urban roadway bridges for maintenance and rehabilitation actions based on multi-attribute utility theory. Four main factors were defined for the bridge maintenance prioritization model. These factors involved destruction and environmental, destruction losses, funds, logistic and information, and strategic and condition. The weights of the sub-factors of the structural condition indicator were computed based on the analytical hierarchy process.

It is worth mentioning that most of the prioritization and maintenance optimization models are deterministic and don't model the inherent uncertainties of the construction process, which usually don't lead to optimal solutions (Mao et al., 2020; Wu et al., 2017). Also, some of the maintenance prioritization models were mainly driven by preferences of domain experts and subjective rankings, which may not be necessarily applicable to be generalized to be applied elsewhere (Safa et al., 2014; Jahan et al., 2012). Most of the previous studies relied on historical records to determine the cost of the maintenance actions, which are not necessarily accurate and may not fit the case in hand (Bukhsh et al., 2020; Mahdi et al., 2019). The absence of precise and resource-driven cost estimation models can heavily influence the decision-making process at different levels of management (Zhang et al., 2008). It is noted that bridge deck replacement has been rarely investigated within the state of the art despite its criticality from technical, economic and social aspects.

Although environmentally conscious construction has been explored in the last decade (Hansen and Sadeghian, 2020; Ozcan-Deniz and Zhu, 2015), there is lack of studies which analyzed the multi-objective optimization of construction projects accounting for time, cost and environmental impact perspectives during the initial planning phases. These models are required

to provide efficient planning, evaluation and selection of the construction equipment. In the last two decades, several simulation-based optimization frameworks were designed for resource allocation of different construction processes. The simulation-based models are characterized by their complex nature and the presence of large number of activities coupled with the presence of wide resource combinations exhibit a more complex behavior. This high computational complexity results in a highly computational expensive model. Additionally, it may lead to slow convergence and inferior solutions resulting from the need to explore this large hyper search space (Parnianifard et al., 2019; Chen et al., 2019**)**. Another shortcoming of some of the simulation-based optimization models is the lack of practicality as a result of the absence of user friendly and computational efficient automated paradigm to facilitate its implementation by users. Another aspect to consider is that the most of the resource allocation models employed genetic algorithm to search for the optimum solutions. Nevertheless, the use of genetic algorithm is often criticized by the low exploration and exploitation capacity, which leads to the entrapment in local minima rather than the true optimal solutions (Jin 2011; AlSukker et al., 2010).

3. PROPOSED METHOD

The main objective of the present study is to introduce an automated platform for modeling and optimizing the performance aspects and utilization rates of limited resources in bridged deck replacement projects. The developed integrative evolutionary-based method is divided into three models namely, discrete event simulation, machine learning and multi-objective optimization (see Figure 1). In the first model, the bridge deck replacement is modeled using STROBOSCOPE simulation platform. The outcomes of this model encompass the performance aspects of time, cost and greenhouse gases for the different resource allocation

plans alongside the utilization rates of resources in the different phases. This output depends on the different input scenarios of resource allocation plans that include diverse and wide-ranging combinations for the numbers of each type of resources. Martinez (1996) introduced STROBOSCOPE simulation engine to model resourced-based complex operations in diverse fields based on discrete event simulation. It is advised by many researchers because of its programming-based nature, which gives the elements a unique behaviour that provides higher degree of flexibility and extensibility than graph-based simulation platform such as EZStrobe. The first step is to define the logic, constraints, resources and the activities that support the logical sequence required for the bridge deck replacement.

STROBOSCOPE is capable of accommodating both deterministic and stochastic input variables. Stochastic modeling of the input variables in simulation models is an acceptable approach that have widely used by several research studies to mimic and approximate the actual performance (Khetwal et al., 2020; ; Zhang, 2015; Thipparat et al., 2013; Lee et al., 2012), especially when taking into consideration that there are lack of models reported in the literature which can look at the actual performance of different combinations of resources in bridge deck replacement projects as highlighted in the “Literature Review” section. The productivity rates and direct costs are based on the historical data published in the RSMeans Building Construction Cost Data 2017 (Gordian RSMeans Data, 2017). The fuel consumption rates of the involved construction equipment are adopted from Caterpillar Inc. (2013). Rsmeans Building Construction Cost Data 2017 is used to capture the average and most commonly experienced productivity rates under normal conditions and eight-hour work day (Yun et al., 2012; Lewis and Hajji, 2012). They are based on actual data collected from wide range of projects, common construction practices and international construction manuals. RSmeans is a widely accepted resource to retrieve the most

likely values of the crew-based productivity data. It has been successfully utilized as an input for simulation-based models in several applications such as cost and time analysis of digital fabrication (García de Soto et al., 2018), assessment of workers' muscles fatigue on construction operations (Seo et al., 2016), studying environmental emissions in buildings (Inyim et al., 2016; Rasdorf et al., 2012), analyzing learning curve on productivity rates (Shehwaro et al., 2016), and modeling construction earthmoving operations (Zankoul et al., 2015). Caterpillar performance books have been adopted by researchers to obtain the hourly fuel consumption rates of different equipment models (Hasan et al., 2020; Yi et al., 2017; Dindarloo and Siami-Irdemoosa, 2016; Jassim et al., 2016).

The captured productivity rates and fuel consumptions are then modelled as stochastic distributions in order to capture the inherent uncertainties, unforeseen conditions and impreciseness associated with the construction processes at the operational level. The productivity rates of the resources and the hourly fuel consumption rates are assumed to follow normal distribution (Kim et al., 2018; Younes et al., 2020; Puri et al., 2013; Marzouk and Younes, 2013) and triangular distribution (Poonthalir and Nadarajan, 2018; Kim et al., 2016), respectively. The distributions are used by previous studies due to their simplicity in analytical computations, generality and efficient representation of the stochastic nature of the input variables in the discrete event simulation model. After running the STROBOSCOPE simulation engine, the designated fields from the output report are stored in applicable readable Microsoft Excel format for further analysis. This comprises the involved resources in each phase, average utilization factor, standard deviation factor, time, cost and greenhouse gases. The resulting output variables of the performance aspects and utilization rates of resource allocation are represented in the form of normal distributions. In this regard, mean is acceptable in terms of computational

complexity and accuracy. The mean of the output distributions is computed to be used as an input for the subsequent computational procedures. The simulation was run 328 times with different resource combination scenarios yielding 328 output files. The Microsoft Excel output files were combined, mapped and appended into the relevant database field.

The main objective of the second model is to design an efficient, practical and straightforward surrogate machine learning model to mimic the computationally exhaustive discrete event simulation model within an acceptable accuracy. In this regard, the data-driven machine learning is designated for simulating automatically the performance aspects of time, cost and greenhouse gases for the different resource allocation plans in addition to their utilization rates. This comprises two stages, whereas the first surrogate model aims at predicting the efficiency and balance in the utilization of resources based on the number of utilized resources. In the first machine learning model, the numbers of resources are the input neurons while the output neurons are the utilization rates of resources in each phase. The efficiency and uniformity of utilization of resources is evaluated according to unified metrics that aggregate the utilization rate of resources used in each phase. Then in the second stage, the utilization rates alongside with the number of resources are fed into another machine learning model to forecast the time, cost and greenhouse gases. In the second machine learning model, the input neurons are the number and utilization rates of resources in each phase. The output neurons are the time, cost and greenhouse gases associated with each resource allocation plan. In this manner, the performance aspects of the resource allocation are evaluated based on the number and time spent by resources in their respective activities.

The proposed model utilizes a hybridization of Elman recurrent neural network (ENN) and invasive weed optimization (IWO) algorithm to enhance the prediction accuracy of simulating

the afore-mentioned predictors. Training Elman neural networks with meta-heuristic optimization algorithms is a powerful mechanism to improve the search engine of the Elman neural network by addressing the exploration-exploitation trade-off dilemma. The proposed model utilizes invasive weed optimization algorithm for both parametric and structural learning, i.e., to automatically optimize the weights and define the best possible architecture of the Elman recurrent neural network. Invasive weed optimization algorithm is selected as a training mechanism because it manifested its efficacy in dealing with different and complex problems including operation of reservoir systems (Azizipour et al., 2016), waste management (Tirkolaee et al., 2019), and surface defects detection (Mohammed Abdelkader et al., 2020). Additionally, it outperformed a set of widely-acknowledged meta-heuristics such as genetic algorithm, particle swarm optimization algorithm, improved particle swarm optimization and shuffled frog-leaping (Prabha et al., 2016; Saravanan et al., 2014). The Elman neural network is trained by designing a variable-length single-objective optimization problem which encompasses a fitness function of minimization of mean absolute percentage error. The steps of the invasive weed optimization algorithm are repeated until satisfying the convergence criteria, i.e., reaching maximum number of iterations. The optimized Elman neural network is appended and utilized to simulate the testing dataset.

The surrogate machine learning model is validated through three phases. The purpose of the first phase is to evaluate the statistical significance of the output of the discrete event simulation model and the machine learning model using Shapiro-Wilk test of normality and Mann-Whitney-U test. This is done to experiment if the machine learning model can efficiently mimic the discrete event simulation model. The second phase involves its comparison with nine conventional prediction models reported for their higher accuracies, namely back-propagation

artificial neural network (ANN), radial basis neural network (RBNN), generalized regression neural network (GRNN), convolutional neural network (CNN), linear kernel support vector machines (LSVM), radial kernel support vector machines (RSVM), gradient boosted decision trees (GBDT), Gaussian process (GP) and K-nearest neighbors ($K-NN$). Their performances were evaluated as per mean absolute error (MAE), root-mean squared error (RMSE) and mean absolute percentage error (MAPE). These performance measures are normally used as metrics to evaluate the suitability and accuracy of the predication models (Fayaz et al., 2019; Le et al., 2019; Yahya et al., 2019). Lower values of MAE, RMSE and MAPE imply a better prediction model. It is worth mentioning that the performances were assessed using split validation and 10-fold cross validation. The K-fold cross validation is used to ensure the training and testing of the entire dataset, which truncates any possibility of over-fitting or over-learning in the pattern recognition phase. The third phase incorporates utilizing non-parametric testing to evaluate the statistical significance level of the outcome of prediction models using the performances of the different folds. Non-parametric tests include Wilcoxn test, Mann-Whitney-U test, Kruskal–Wallis test, binomial sign test and Mood's median test.

The third model incorporates building a multi-objective differential evolution paradigm to optimize the resources based on the total project duration, total project cost and total greenhouse gases, and subject to the targeted average and dispersion in the utilization of the consumed resources. In this model, the calibrated machine learning models of the previous stage are utilized herein as fitness functions and terms of objective functions. Differential evolution algorithm is exhaustive search engine that demonstrated higher exploration and exploitation capacities in investigating higher-dimension and multi-local spaces (Yagiz et al., 2020; Yu et al., 2018). Furthermore, it proved its efficiency in dealing with various and exhaustive search

problems such as design of reinforced concrete continuous foundation (Kamal and Inel, 2019), stream flow simulation (Al-Sudani et al., 2019) and design of net zero buildings (Chai et al., 2020). It is validated through comparisons with a set of well-performing state of the art meta-heuristics, namely multi-objective genetic algorithm (MOGA), multi-objective particle swarm optimization algorithm (MOPSO), multi-objective dragonfly algorithm (MODA), multi-objective grey wolf optimization algorithm (MOGWO), multi-objective Jaya algorithm (MOJAYA) and multi-objective shuffled frog-leaping algorithm (MOSFL). Additionally, the developed multi-objective optimization model is compared against non-linear programming that uses Levenberg-Marquardt algorithm.

The comparisons of optimization models were conducted as per a set of performance indicators, which included average fitness function values, coefficient of variation of fitness function values, hypervolume indicator, generational distance, spacing, diversity, spread and coverage. These performance metrics are capable of evaluating three main aspects which are: diversity, accuracy and cardinality (Cui et al., 2020; Falahiazar and Shah-Hosseini, 2018; Chen et al., 2018). Then, the significance levels of the optimal solutions of the different meta-heuristic optimization algorithms are evaluated using non-parametric testing. Multi-criteria decision making is performed to identify the most feasible solution among the set of Pareto optimal solutions. Shannon entropy is employed to compute the weights of the attributes. Subsequently, Preference Ranking Organization Method for Enrichment Evaluations (PROMETHEE II) is utilized to rank the Pareto optimal solutions according to the net outranking flow. The net outranking flow evaluates the different resource allocation plans collectively according to their time, cost and greenhouse gases. PROMETHEE II is selected over other multi-criteria decision making approaches because of its robustness and efficiency in solving multi-attribute decision problems

in diverse fields including optimal site selection of parabolic tough concentrating solar power plant (Wu et al., 2019), sustainability assessment of large scale composite technologies (Makan and Fadili, 2020), and ranking of sub-watersheds threatened by erosion process (Vulević and Dragović, 2017). The previous models are automated using a computerized platform that encompasses a hybridization of C#.net and Matlab programming languages. It is expected that the automated platform is capable of exploiting the compatibility and versatility capabilities of C#.net and the superior computational capacity of the Matlab.

INSERT FIGURE 1

4. METHOD DEVELOPMENT

This section describes in detail the three main models reported in the "Proposed Method" section.

4.1 Discrete Event Simulation Model

As early mentioned, the proposed simulation model is developed using STROBOSCOPE in order to capture the sequences of the involved tasks in the bridge deck replacement process. Figure 2 depicts the simulation network of the bridge deck replacement process. The STROBOSCOPE simulation elements, which are used to model the involved tasks in the simulation process, are depicted in Table 1. The simulation elements include: Queue, Link, Normal, Combi and Consolidator. The simulation model starts by demolishing the existing bridge deck. Then, the demolished segment is loaded into the trucks by the loaders. The trucks then travel and dump the demolished segment and travel back to be loaded again by the loaders. This process continues until reaching the desired number of segments to be demolished. The second phase is the construction phase, whereas the stepping shuttering system is assembled then

it is pushed hydraulically until erected on an existing bridge pier. Afterwards, the stepping shuttering advances into its position using a group of hydraulic jacks.

The utilized construction method is for a pre-stressed concrete bridge, in which the tendons are tensioned before the concrete is placed. The bridge deck is casted on two stages: the first stage is casting the bottom slab and the second stage is casting the web and top slab. The formwork of the bottom slab is erected then the tendons are placed in a prescribed pattern on the casting bed between two anchorage systems. After that, the tendons are tensioned using hydraulic jacks to a value that should not exceed 94% of the specified yield strength nor 80% of the strength of the pre-stressing steel nor the maximum value recommended by the manufacturer of the steel. Finally, the concrete is casted and allowed to cure. The same previous steps are repeated for casting the web and the top slab. The whole construction process is replicated till reaching the desired number of segments to be casted.

The final phase is the finishing phase, which starts by installing the curbs then laying the asphalt layers. The first layer of the asphalt is the aggregate base course layer, which is compacted and spread on two layers, whereas each one of them is 15 cm. Then, the aggregate base course layer is tested to ensure that it meets the desired specifications. Subsequently, the prime coat (MC-30) is spread using tankers and tested. Then, the asphalt binder course is spread using finishers and compacted using rollers and then tested. The tack coat (RC-70) is then spread using tankers and tested. Finally, the final asphalt pavement course layer is spread, compacted and tested. The sidewalks are then installed and finally the epoxy pavement markings are placed

The total duration, cost, greenhouse gases of the project in addition to the utilization factors of the different resources are computed in the STROBOSCOPE simulation engine to build the

machine learning database. These performance aspects and utilization rates are computed according to the values of productivity rates of resources, hourly fuel consumption rates, daily direct cost of the resource, average consumption of equipment, carbon emission factor and density of diesel. Different and wide-ranging combinations of resources are created and their respective performance aspects and utilization rates are computed. These values are appended and used as an input to the subsequent surrogate machine learning model.

INSERT FIGURE 2

INSERT TABLE 1

4.2 Surrogate Machine Learning

Simulation models usually invoke numerous iterations, which result in lengthy processing times and CPU intensive simulation process. As such, a surrogate model needs to be developed and calibrated to circumvent the shortcomings of the computational time-expensive nature of the discrete event simulation model. Surrogate models are sometimes known as emulators, meta models, proxy models, low fidelity models, reduced models or response surface models. The main advantage of the surrogate models is that it capitalizes on the empirical relationships to imitate the input-output behavior of the discrete event simulation process within less computational time and acceptable computational accuracy. In this regard, the developed surrogate machine learning model is trained and tested using the output generated from the discrete event simulation model. Once the surrogate model is calibrated and validated, the input variables can be directly fed into it to generate the model outcomes within faster computational time. These outcomes are invoked as the multi-objective optimization functions and the set of condition constraints (Mahmoodian et al., 2018; Song et al., 2018).

In the present study, a novel hybrid ENN − IWO is introduced as a surrogate model to evaluate the resource allocation plans of bridge deck replacement process. The developed computer aided application enables their automated assessment from time, cost and environmental perspectives alongside their utilization rates. The developed data-driven machine learning model encompasses two stages. In the first stage, the numbers of resources in each phase are used as an input to forecast the average and standard deviation of utilization rates of resources. In the second stage, the number and utilization rates of resources serve as an input to the machine leaning model for the purpose of predicting the time, cost and amount of greenhouses gases of the different resource allocation plans. In this regard, the utilization rates are adopted for the purpose of capturing the time consumed by resources in a certain construction activity. It should be mentioned that the two stages involves nine ENN − IWO models designated for the prediction of average and standard deviation of utilization of resources alongside the performance aspects of the different resource allocation plans.

Each one of the nine ENN − IWO models is composed of different architecture in terms of numbers of input neurons, hidden and context layers, hidden and context neurons and output neuron. In this context, number of input neurons is equal to the number of input variables. Figure 3 depicts the architecture of the developed ENN − IWO model for the prediction of average utilization rate of resources in the demolition phase ($\mathrm{AVG\_UTIL_{DEM}}$). It is composed of three input neurons for the numbers of hydraulic hammers, loaders and trucks. It is worth mentioning that the developed ENN − IWO model for the prediction of the performance aspects of resources allocation plans is composed of 20 input variables. The input variables are adopted from the literature so that they cover all utilized resources alongside the average and standard deviation of utilization of resources in each phase separately of bridge deck replacement process. In this

manner, the selection of input variables is capable of considering both the number of resources and the time spent by them. The input variables encompass numbers of hydraulic hammers, loaders, trucks, form crews, rebar crews, stress crews, concrete crews, finishing crews, graders, rollers, tankers, finishers, sidewalk finishing crews and painting crews. They also include average and standard deviation in the utilization of resources in demolition phase, construction phase and finishing phase.

INSERT FIGURE 3

In the developed surrogate machine learning model, invasive weed optimization is used as a training engine in an attempt to amplify the search capacity of the training mechanism through deriving the optimum weights and configuration of the Elman neural network. The Elman neural network is coupled with invasive weed optimization algorithm to alleviate the drawbacks of the derivative-based back propagation training algorithms and low computational efficiency resulting from the manual tuning of the parameters of Elman neural network. The training process based on the gradient descent usually gets trapped in a local minima or premature convergence and sometimes causes over-fitting problems mostly in the presence of multilayer neural network (Shreyas and Dai, 2020; Jabin, 2014). The second reason is the existence of wide range of parameters, which substantially affect the performance of the neural network. This includes initial setting of weights, numbers of hidden and context layers, number of hidden and context neurons and types of transfer function. These parameters are sensitive to their initial values, whereas their initial setting is always variable from one case to the other. In this context, the blindness in the determination of such parameters can result in the network to be trapped in an inferior solution and subsequently a long computational time of the training process and slow convergence (Zhang et al., 2020). Thus, a self-adaptive model is designed in order to tune

automatically and dynamically its parameters and hyper parameters based on the available dataset generated from the discrete event simulation model.

The developed $\mathrm{ENN-IWO}$ model involves both structural and parametric learning. In this regard, an invasive weed optimization algorithm is adopted to optimize the hyper parameters of Elman neural network and the weight connections between neurons. The structural learning involves find the optimum architecture of Elman neural network, which encompasses optimum number of hidden layers, number of context layers, number of hidden neurons, number of context neurons and transfer function. The present research study investigates eight types of transfer activation functions, namely hyperbolic tangent sigmoid transfer function, Elliot symmetric sigmoid transfer function, log-sigmoid transfer function, linear transfer function, positive linear transfer function, radial basis transfer function, triangular basis transfer function and normalized radial basis transfer function.

Elman neural network is one of the recurrent neural networks (RNNs), which was proposed by Jeffrey Locke Elman in 1990. Elman neural network is characterized by additional context layers, which helps in providing a memory about the results of the computations done so far. This behaviour enables the neural network to maintain short term memory, which improves the network performance (Köker, 2013; Wang et al., 2014). The training process of the Elman neural network is performed based on a single objective function which minimizes the mean absolute percentage error of the different performance indicators as shown in Equation (1).

$$\mathrm{MAPE} = \frac{100}{\mathrm{k}} \times \sum_{\mathrm{i}=1}^{\mathrm{K}} \frac{|\mathrm{PR_i} - \mathrm{AC_i}|}{\mathrm{AC_i}} \tag{1}$$

Where;

AC_i, PR_i stand for the actual and predicted values, respectively. The actual and predicted values are either duration, cost, greenhouse gases or the unified utilization factor of resources. K represents the number of data points. It is worth noting that the mean absolute percentage error is selected because it is a well-recognized good performing performance indicator, unitless, and un-biased performance metric. Additionally, it is usually more practical and efficient to deal with cost functions, i.e., error functions.

The developed $\mathrm{ENN}-\mathrm{IWO}$ model involves structural learning. As such, the number of weights and bias terms vary iteratively during each training epoch as per the numbers of hidden layers, hidden neurons, context layers and context neurons. As mentioned earlier, IWO algorithm is employed to train the Elman neural network. In this regard, the length of the optimization model is varying according to the Elman neural network's hyper parameters. In this context, an estimator is designed for the purpose of modeling the dynamism and the variability in the length of the optimization model taking into consideration the possibility of presence of multi-hidden layer and multi-context layer Elman neural network. This estimator enables the computation of number of weights and bias terms in each training epoch as follows.

$$\mathrm{Num} = \big((\mathrm{I}+1)\times \mathrm{N}\big) + ((\mathrm{N}\times \mathrm{C}\times \mathrm{P} + (\big(\mathrm{N}+1)\times \mathrm{N}\times(\mathrm{P}-1)\big) + \big((\mathrm{N}+1)\times \mathrm{O}\big) \qquad (2)$$

Where;

Num represents the total number of weights and bias terms. I represents the number of input neurons. N indicates the number of hidden neurons. C represents the number of neurons in the context layer. P represents number of hidden and context layers. O depicts the number of output neurons. For simplification purposes, the number of context layers is assumed to be equal to the number of hidden layers.

4.3 Multi-objective Optimization Model

In the bridge deck replacement process, so many resources, decision variables and constraints are involved. In this regard, a multi-objective differential evolution model is formulated to identify the optimum number of each resource type such as number of reinforcement crews, number of graders, number of compactors, number of tankers, number of finishers, etc. The nine $ENN-IWO$ models established and calibrated from the previous stage, serve as objective functions, terms of objective functions and constraints. The input and output of the developed multi-objective optimization model are recorded in Table 2. The developed computer aided application gives the user the flexibility to adjust some of the values of the input variable. The optimal resource allocation plan encompasses the optimum number of each type of resources. The solution structure of the multi-objective resource allocation model is depicted in Figure 4. As shown in Figure 4, the search agent or the candidate solution is structured in the form of a string or vector of elements, whose length denotes the number of decision variables of the multi-objective optimization model. The variable X_{ij} takes integer values range from the minimum allowable number of resources to the maximum allowable number of resources. The length of the vector of decision variables is equal to fourteen, such that this vector encompasses numbers of hydraulic hammers, loaders and trucks in the demolition phase. It also involves numbers of form crews, rebar crews, stress crews and concrete crews in the construction phase. For the finishing phase, it incorporates numbers of finishing crews, graders, rollers, tankers, finishers, sidewalk finishing crews and painting crews. The optimal number of each type of resources is represented as vector of solutions. In this regard, it is obtained capitalizing on minimizing the project duration, project cost and project greenhouse gases as shown in Equations (3), (4) and (5), respectively and satisfying the explicit boundary constraints. The constraints are

added to ensure the appropriate efficiency and uniformity (balance) in the utilization of resources as presented in Equations (6) and (7).

$$T_S = \text{Min}\,[\xi\,(R_r, P_r)], \text{for all } r \in \{1,2,3,4 \ldots \ldots . . C\_R\} \quad (3)$$

$$C_m = \text{Min} \sum_{r=1}^{R} R_r \times DC_r \times T_r, \text{for all } r \in \{1,2,3,4 \ldots \ldots . . C\_R\} \quad (4)$$

$$GHG_m = \text{Min} \sum_{e=1}^{E} \text{Cons\_Avg}_e \times \gamma_{\text{Diesel}} \times CEF \times R_e \times T_e, \text{for all } e \in \{1,2,3,4 \ldots \ldots . . E\} \quad (5)$$

Subject to;

$$UNI_{AVG\_UTIL} = \frac{\sum_{p=1}^{PH} \sum_{r=1}^{N} UT\_F_{rp}}{C\_R} \geq C \quad (6)$$

$$UNI_{STD\_UTIL} = \frac{\sum_{p=1}^{PH} STD\_UTIL_p}{PH} \leq B \quad (7)$$

Such that;

$$STD\_UTIL_p = \sqrt{\frac{\sum_{r=1}^{N} \left(AVG\_UTIL_p - UT\_F_r\right)^2}{P\_R}} \quad (8)$$

Where;

T_S, C_m and GHG_m stand for the normalized time, normalized cost and normalized greenhouse gas emissions. The time is measured per span while cost and greenhouse gases are measured per square meter. ξ is an operator which represents the STROBOSCOPE simulation engine. R_r and P_r represent the number of each type of resource and productivity rate of resources, respectively. DC_r indicates the daily direct cost of the resource. T_e represents the actual time spent by the resources in order to consider the idle periods consumed in construction site. E refers the fuel-

based resources. R_e stands for the number of each fuel-based type of resources. $Cons\_Avg_e$ is hourly fuel consumption of certain equipment (liters/hour). γ_{Diesel} is density of diesel such that it is assumed 0.832 Kg/l. CEF_e represents the carbon emission factor for diesel, whereas is assumed 3 Kg CO_2-Eq/Kg (Flower and Sanjayan, 2007). UT_F_{rp} stands for the utilization rate of the resource r in the phase p. UNI_{AVG_UTIL} represents the unified average utilization rate of resources. STD_UTIL_p stands for the standard utilization rate of phase p. UNI_{STD_UTIL} represents the unified standard deviation of utilization rate of resources and it is computed as the average of standard deviation of resources in each phase. AVG_UTIL_p and STD_UTIL_p are the average utilization rate and standard deviation of utilization rate of resources in phase p, respectively. They are computed based on the idle time of crews. C_R indicates total number of type of resources in the project. In the present study, fourteen different types of resources are utilized. N and PH stand for the total number of resources in each phase and total number of phases, respectively. P_R stands for number of types of resources involved in phase p. For instance, demolition phase involves three different types of resources. C and B are threshold values to manage the utilization of resources on site. The developed computer aided application gives the user the flexibility to determine the lower and upper bounds of resources alongside the threshold values. The optimum resource allocation plan is the one which attains least time per span, unit cost and greenhouse gases footprint while maintaining efficient and balanced utilization of resources.

INSERT TABLE 2

INSERT FIGURE 4

Differential evolution (DE) algorithm is an optimization algorithm that was introduced by Storn and Price back in 1997 to search for the global solution of non-linear problems with non-differentiable objective functions (Storn and Prince, 1997). The framework of the differential evolution algorithm is similar to the genetic algorithm. However, the classical mutation and crossover in the genetic algorithm are replaced by alternative mutation and crossover operators. Differential evolution algorithm encompasses five main stages which are: initialization, mutation, crossover, selection, and convergence criteria. Differential evolution algorithm starts by generating a population of D-dimensional parameter vectors (candidate solutions) of size NP. The basic computational procedures of the DE algorithm are as follows (Storn and Prince, 1997; Hamza et al., 2018; Seyedpoor et al., 2015). The generation of individuals can be obtained using the following Equation.

$$X_{i,G} = LB + \mathrm{rand}[0,1] \times (UB - LB) \quad (9)$$

Where;

i denotes the population. G denotes the generation to which the population belongs to. LB, and UB represent two vectors of upper and lower bound for any decision variable, respectively. $\mathrm{rand}[0,1]$ represent a uniformly distributed random number between 0 and 1.

The next step is the mutation, whereas the mutation vector is defined based on the combination of three randomly selected vectors. A vector in the current population is selected to be the target vector (parent). For each target vector ($X_{i,G}$) in the population, a mutant vector is created using the following Equation.

$$V_{i,G+1} = X_{r1,G} + F(X_{r2,G} - X_{r3,G}) \qquad r1 \neq r2 \neq r3 \quad (10)$$

Where;

r1, r2, and r3 represent three random and different indices between 1 and NP. The three random chosen vectors have to be different than the target vector. $V_{i,G+1}$ is the newly created mutant vector. F represents a mutation scale factor that control the amplification of differential variation between $X_{r2,G}$, and $X_{r3,G}$. Mutation scale factor is a real number between [0, 1].

Crossover is performed to diversify the current population by exchanging components of the target vector and the mutant vector. The trial vector (offspring) can be obtained using Equation (11). If the crossover rate is smaller than the random number, $V_{j,i,G+1}$ in the mutant vector is copied to the trial vector. Otherwise, $X_{j,i,G}$ in the target vector is copied to the trial vector.

$$U_{j,i,G+1} = \begin{cases} V_{j,i,G+1} & \text{if } CR \geq rand_j \\ X_{j,i,G}, & \text{if } CR < rand_j \end{cases} \quad (11)$$

Where;

CR represents crossover probability. $U_{j,i,G+1}$ represents trial vector. j represents index element for any vector. $rand_j$ denotes uniform random number between [0,1].

In the selection stage, the trial vector is compared with the target vector to determine if trial vector should be a member of the next generation $G + 1$ as shown in Equation (12). Assume the objective function to be minimized. The vector with lower objective function survives to the next generation. If the trial vector yields a lower objective function than the target vector, then the trial vector replaces the target vector in the next generation.

$$X_{i,G+1} = \begin{cases} U_{i,G+1} & \text{if } f(U_{i,G+1}) \leq f(X_{i,G}) \\ X_{i,G}, & \text{if } (U_{i,G+1}) > f(X_{i,G}) \end{cases} \quad (12)$$

Mutation, crossover, and selection are repeated in each generation until stopping criterion is satisfied, i.e., reaching maximum number of generations.

4.4 Multi-criteria Decision Making

The objective of the multi-criteria decision making model is to select the best resource allocation plan among Pareto optimal solutions obtained from the multi-objective optimization model. In this regard, Shannon entropy algorithm is applied for the computation of the weighted importance vector of time, cost and greenhouse gases. PROMETHEE II is then employed to rank the resource allocation plans capitalizing on their duration, cost and produced greenhouse gas emissions. Shannon entropy is an objective weighting algorithm that relies on the decision matrix to derive the weighting importance of attributes in an attempt to alleviate the limitations of subjective preference-based weighting algorithms. Entropy is a measure of randomness and uncertainties of information demonstrated by discrete probability distribution, whereas larger amount of information implies smaller uncertainties and entropy values, which indicates that the attribute has higher importance. Entropy can be also utilized to evaluate the degree of dispersion of alternatives associated with a given attribute. In this regard, a higher degree of dispersion implies a greater relative importance of the attribute. The computational procedures of the Shannon entropy algorithm can be summarized as follows (Wu and Hu, 2020; Hafezalkotob and Hafezalkotob, 2015).

The first procedure is the normalization of the performance indices in the decision matrix which is accomplished using Equation (13).

$$P_{ij} = \frac{x_{ij}}{\sum_{i=1}^{m} x_{ij}} \quad (1 \leq i \leq m, 1 \leq j \leq n) \tag{13}$$

Where;

P_{ij} represents the projection value of the $i-th$ alternative with respect to $j-th$ attribute. x_{ij} represents the measure of performance of the $i-th$ alternative with respect to $j-th$ attribute. The terms m and n indicate the number of alternatives and number of attributes, respectively.

The second procedure involves the computation of entropy value for each criteria using Equation (14)

$$e_j = -k * \sum_{i=1}^{m} P_{ij} * \ln P_{ij} \ (1 \leq i \leq m, 1 \leq j \leq n) \quad (14)$$

Where;

e_j refers to the entropy value of the $j-th$ attribute, and $k = \frac{1}{\ln(m)}$.

The third procedure encompasses the computation of the degree of dispersion of intrinsic information for different attributes using Equation (15).

$$d_j = 1 - e_j \quad (15)$$

Where;

d_j denotes the inherent contrast intensity or dispersion of attribute j, whereas a higher value of d_j indicates more relative importance assigned to the attribute j.

The objective weigh of each attribute can be computed using Equation (16).

$$w_j = \frac{d_j}{\sum_{j=1}^{n} d_j} \quad (16)$$

Where;

w_j denotes the relative importance weighting of the $j-th$ attribute.

The family of PROMETHEE approaches were developed by Brans and Vincke (1985) to enable decision makers to establish a ranking of a finite set of alternatives. It is an outranking multi-criteria decision analysis approach that can be applied to generate partial ranking of alternatives (PROMETHEE I) or full ranking of alternatives (PROMETHEE II). A preference function is assigned for each attribute, which enables to determine how much alternative a is preferred over alternative b through mapping the differences in the evaluation of the two alternatives. The preference degrees in the preference functions are represented in a numerical scale ranging from zero to one, whereas one indicates that alternative a is strongly preferred over alternative b while zero implies indifference preference value between the two alternatives a and b. There are six different types of preference functions including usual criterion, U-shaped (Quasi) criterion, V-shaped criterion, level criterion, V-shaped with indifference (linear) criterion and Gaussian criterion.

In these preference functions, the indifference threshold and preference threshold need to be identified. Indifference threshold (Q) represents the largest deviation that is considered as negligible by the decision maker. Preference threshold (P) denotes the smallest deviation that is regarded as sufficient to generate full preference for the decision maker. A Gaussian threshold (S) is used only in the case of Gaussian preference function. The Gaussian threshold is usually an intermediate value between the indifference threshold and preference threshold. In the present study, V-shaped preference function is selected for the attributes of time, cost and greenhouse gases. It is selected because of its efficiency in dealing with quantitative nature of the present data, which enables to establish a clearer distinction between the evaluations of alternatives. Furthermore, it requires less parameters to be tuned (Brankovic et al., 2018; Kolios et al., 2016). The preference threshold value of each attribute is assumed 60% of the difference between the

maximum and minimum performance evaluation (Gervásio and Simões da Silva, 2012). The basic procedures of applying PROMETHEE II are adopted from Brans et al. (1986). In it, the ranking of the resource allocation plans is carried out using the net outranking flow. A higher value of net ranking outranking flow implies a better resource allocation based on a collective evaluation performance of their respective time, cost and greenhouse gases.

5. MODEL IMPLEMENTATION

The case study is for a bridge that is composed of 8 lanes and 20 spans. The length of the span and width of the lane are 20 and 3.75 metres, respectively. The width of the sidewalk is 3 metres. All the computations took place on a laptop with an Intel Core i7 CPU, 2.2 GHz and 16 GB of memory. Table 3 describes the lower and upper bounds for the output variables of the discrete event simulation model that were used to generate the machine learning surrogate model. The output variables include: time per span (T_S), cost per square meter (C_m), greenhouse gases per square meter (GHG_m), average utilization rate of demolition phase (AVG_UTIL_{DEM}), and standard deviation of utilization rate of demolition phase (STD_UTIL_{DEM}), average utilization rate of construction phase (AVG_UTIL_{CONST}), standard deviation of utilization rate of construction phase (STD_UTIL_{CONST}), average utilization rate of finishing phase (AVG_UTIL_{FINISH}) and standard deviation of utilization rate of finishing phase (STD_UTIL_{FINISH}). For instance, the lower and upper bounds of the output variable GHG_m are 11.214 and 24.047, respectively.

INSERT TABLE 3

The next phase is to build the surrogate machine learning model using the simulation dataset to construct a reliable approximation of the STROBOSCOPE model. It is worth mentioning that the output variables T_S, C_m and $GHG_m$are computed using the number of involved resources in

addition to the variables $\text{AVG\_UTIL}_{\text{DEM}}$, $\text{STD\_UTIL}_{\text{DEM}}$, $\text{AVG\_UTIL}_{\text{CONST}}$, $\text{STD\_UTIL}_{\text{CONST}}$, $\text{AVG\_UTIL}_{\text{FINISH}}$, and $\text{STD\_UTIL}_{\text{FINISH}}$ in order to account for both the number of resources and the time spent by them. The surrogate model is the $\text{ENN} - \text{IWO}$ that capitalizes on the invasive weed optimization algorithm to identify the optimum topology of the Elman neural network alongside its optimum characteristics. With respect to the prediction of cost and greenhouse gases, the user can specify the lower and upper bounds for the different structural and parametric learning parameters in addition to the parameters of the invasive weed optimization algorithm. The user interface of the automated prediction of greenhouse gases footprint is depicted in Figure 5. As shown in Figure 5, the maximum numbers of hidden layers and hidden neurons are equal to 10. Thus, the maximum lengths of the optimization problem are 2214 for both cost and greenhouse gases. This is considered as a large search space that substantiates the employment of exhaustive training mechanism. The parameters of the IWO algorithm are as follows: the number of iterations and the initial population size are assumed 500 and 250, respectively. The maximum and minimum numbers of seeds are 5 and 0, respectively. The initial and final standard deviations are assumed 0.5 and 0.001, respectively. The non-linear modulation index is two.

INSERT FIGURE 5

For the cost prediction model, the optimum numbers of hidden and context layers are four while their optimum numbers of hidden and context neurons are four also. Elliot symmetric sigmoid is the optimum transfer function. In the cases of greenhouse gases prediction model, the optimum structure is composed of three hidden and context layers in addition to six hidden and context neurons. Furthermore, Elliot symmetric sigmoid is the optimum transfer function. The convergence curves of the mean absolute percentage error for greenhouse gases and cost are depicted in Figures 6 and 7, respectively. As shown in Figures 6 and 7, the least mean absolute

percentage errors achieved by the invasive weed optimization algorithm for greenhouse gases and cost are 6.333% and 2.359%, respectively. This manifests the superior capacity of the invasive weed optimization algorithm in solving complex and variable-length optimization problems.

INSERT FIGURE 6

INSERT FIGURE 7

The validation process of the surrogate model is three-folded. The first fold is to ensure that the surrogate machine learning model can efficiently substitute the discrete event simulation model. Shapiro-Wilk test is applied to study the normality of the data at significance level (α) of 0.05. It examines the null hypothesis (H_0), which is that the random variable follows a normal distribution. On the other hand, the alternative hypothesis (H_1) assumes that the random variable doesn't follow a normal distribution. As such, if the $P-value$ is less than the significance level, then the null hypothesis is rejected in favor of the alternative hypothesis. Nevertheless, if the $P-value$ is more than the significance level, thus the null hypothesis is accepted. Table 4describes the $P-values$ of the simulation and machine learning models for the different output variables. As presented in Table 4, all the $P-values$ of the discrete event simulation and machine learning models are less than 0.05, which imply that the null hypothesis is rejected and therefore the output variables of both models don't follow normal distribution.

INSERT TABLE 4

In the light of foregoing, a non-parametric Mann-Whitney-U is applied to evaluate the statistical significant differences between the discrete event simulation and machine learning models at a significance level of 0.05 (see Table 5). The performed Mann-Whitney-U test investigates the null hypothesis (H_0), which implies that there are no significant differences between the discrete

event simulation and machine learning models. The alternate hypothesis (H_1) indicates that there are statistical significant differences between the discrete event simulation and machine learning models. The $P-$values of the pairs (Discrete event simulation, machine learning) for all the prediction models are more than 0.05. This means that the null hypothesis is accepted. Thus, there is no statistical significant difference between the discrete event simulation model and machine learning model. Hence, the machine learning model can efficiently substitute the discrete event simulation model for all the output variables.

INSERT TABLE5

The second fold comprises a comprehensive performance comparison between the proposed $ENN-IWO$ model and other conventional machine learning prediction models. Table 6 and Table 7 report performance comparisons between the machine learning models as per split validation for the prediction of cost and greenhouse gases, respectively. Additionally, Table 8 records the performance evaluation metrics of greenhouse gases as per 10-fold cross validation. It is important to mention that 80% (262) and 20% (66) of the dataset are utilized for training and testing the prediction models, respectively. For cost prediction, the proposed model attained the highest prediction accuracy when compared to other prediction models reported in the literature, whereas the $MAPE$, MAE and $RMSE$ are equal to 4.873%, 78.466 and 39.515, respectively. CNN achieved the second lowest $MAPE$ while ANN had the second lowest MAE and $RMSE$. $LSVM$ provided the least performance, whereas $MAPE$, MAE and $RMSE$ equal to 18.361%, 214.525 and 111.639, respectively.

In terms of greenhouse gases, the proposed $ENN-IWO$ model provided the highest performance, such that $MAPE$, MAE and $RMSE$ are equal to 4.873%, 78.466 and 39.515, respectively. $K-NN$, $GBDT$ and $RSVM$ provided the second highest performance according to

MAPE, MAE and RMSE, respectively. GP provided the lowest prediction accuracies, whereas MAPE, MAE and RMSE equal to 24.879%, 5.713 and 4.117, respectively. Back-propagation artificial neural network is the most widely-used algorithm in machine learning applications. when compared against the ANN model in greenhouse gases prediction, the $\mathrm{ENN-IWO}$ accomplished an enhancement in the reduction of MAPE, MAE and RMSE by 44.421%, 46.203% and 40.298%, respectively. With respect to the cross validation, It can be inferred that the proposed $\mathrm{ENN-IWO}$ outperformed the remainder of the machine learning models with respect to three performance indicators attaining; MAPE, MAE and RMSE 7.417%, 1.701 and 1.293, respectively. On the contrary, GP provided the lowest prediction accuracies, such that MAPE, MAE and RMSE are equal to 28.113%, 6.473 and 4.669, respectively. This highlights that the proposed prediction model outperformed other machine learning models by accomplishing lower prediction errors for the different output variables according to split validation and 10-fold cross validation.

INSERT TABLE 6

INSERT TABLE 7

INSERT TABLE 8

The third fold in the validation process is to evaluate the statistical significant differences between the different prediction models based on the output of the different ten folds according to the MAPE. Wilcoxn test, Mann-Whitney-U test, Kruskal–Wallis test, binomial sign test, and Mood's median test of the different cost and greenhouse gases prediction models are shown in Tables 9 and 10, respectively. As can be seen, $\mathrm{P-values}$ of the pairs $(\mathrm{ENN-IWO,\ ANN})$, $(\mathrm{ENN-IWO,\ RBNN})$, $(\mathrm{ENN-IWO,\ GRNN})$, $(\mathrm{ENN-IWO,\ CNN})$, $(\mathrm{ENN-IWO,\ LSVM})$, $(\mathrm{ENN-IWO,\ RSVM})$, $(\mathrm{ENN-IWO,\ GBDT})$, $(\mathrm{ENN-IWO,\ GP})$ and $(\mathrm{ENN-IWO,\ K-NN})$ are

less than 0.05 for all the previously-mentioned statistical tests in both predicting the cost and greenhouse gases. This reveals that there are significant differences in the prediction capacities of the proposed model with respect to other machine learning and deep learning models. In view of the above, it can be stated that the proposed $\mathrm{ENN}-\mathrm{IWO}$ significantly outperformed other nine prediction models.

INSERT TABLE 9

INSERT TABLE 10

The third model is multi-objective differential evolution to find the optimum combinations of resources. Figure 8 depicts the user interface of the multi-objective differential evolution optimization model. In it, the user is asked to define the maximum and minimum number of resources as well as setting the parameters of the differential evolution algorithm. By clicking "View: button, the output of the model is displayed which comprises the optimum solutions (performance design space) and the optimum objective function values (feasible performance space). The maximum number of resources for its different types is set to be 15.. The minimum allowable average utilization rate and maximum allowable standard deviation of utilization rate of resources are assumed 85% and 10%, respectively. This state of affairs necessitates the implementation of efficient meta-heuristic for the purpose of exhaustive search of possible resource allocation plans while accommodating the allowable utilization constraints.

In order to provide a fair comparison between the different meta-heuristic optimization algorithms, the population size and number of iterations are assumed 100 and 100, respectively. Different initializations of parameters were experimented for the different meta-heuristics in order to search for their optimum values. Each meta-heuristic was run ten times independently in order to avoid unstable solutions due to random initialization of population. In the developed

model, the crossover probability is assumed 0.2 while the mutation is assumed to follow a uniform distribution between 0.2 and 0.8. In the genetic algorithm, tournament selection is the parent selection strategy. Two-point crossover is utilized, and the crossover rate is assumed 0.8. Mutation rate is assumed 0.1. For the particle swarm optimization algorithm, the cognitive learning and social parameters are assumed two. The inertia weight is assumed 0.5. For the shuffled frog leaping algorithm, the number of memeplexes is assumed 20, i.e., 5 frogs per each memeplex. In the grey wolf optimization algorithm, the trade-off parameter which controls the balance between exploration and exploitation is assumed to be linearly decreasing from 2 to 0. The constant used to manage the Levy's flight mechanism in the dragonfly algorithm is assumed 1.5. In the Jaya algorithm, the random number utilized to generate new solutions is assumed to be between 0 and 1.

INSERT FIGURE 8

The set of optimal solutions obtained from the multi-objective particle swarm optimization model and multi-objective differential evolution optimization model are depicted in Figures 9 and 10, respectively. The performance design space is defined as the set of all design points represented by the design (decision) variables that satisfy the constraints. The feasible performance space represents the set of objective function values elicited from every feasible design. The non-dominated Pareto optimal solutions attained from the multi-objective particle swarm optimization model and multi-objective differential evolution optimization model are shown in Figures 11.a and 11.b, respectively. As can be seen, the differential evolution algorithm attained notable lower T_S, C_m and GHG_m compared to the particle swarm optimization algorithm.

INSERT FIGURE 9

INSERT FIGURE 10

INSERT FIGURE 11

In order to provide a rigorous and robust comparison between the different multi-objective meta-heuristics, they are evaluated with respect to the average objective function values, coefficient of variation of objective function values hypervolume indicator, generational distance, spacing, diversity, spread and coverage based on the performance of ten independent runs (see Table 11). The values mentioned herein represent the average values for the different performance indicators. The bolded values represent the best achieved performance by the meta-heuristics used in this study. The best performing meta-heuristic optimization algorithm is the one which yields higher values of hypervolume indicator, lower values of generational distance, lower values of spacing, lower values of diversity, higher values of spread and lower values of coverage. Furthermore, a lower coefficient of variation implies more accuracy and higher stability of the meta-heuristic optimization algorithm.

It can be interpreted from Table 11 that non-linear programming (NLP) provided T_S, C_m and GHG_m of 59.026, 1444.287 and 19.549, respectively. This demonstrates that NLP failed to find optimum solutions since it provided higher objective function values than the ones achieved by MODE and other meta-heuristics. In this regard, the current resource allocation optimization problem is $NP-hard$ which stands for non-deterministic polynomial time. This is due to presence of computationally expensive search space resulting from the large number of possible combinations, large number of objective functions, combinatorial nature of optimization problem, and existence of hard constraints that cannot be violated (Le et al., 2019; Su et al., 2018). It is worth mentioning that the search space size of the developed optimization model is computed based on the maximum allowable number of resources in the computer aided application. In this regard, the number of possible solutions as $15^{14} = 2.92 \times 10^{16}$, which

demonstrates that the search space of the developed optimization model is computationally expensive. In this context, exact optimization methods to fail to solve the present $\mathrm{NP}-\mathrm{hard}$ problem and meta-heuristics are applied to search for the near-exact optimal solutions (Petroodi et al., 2019; Bagloee and Sarvi, 2018).

It can be also inferred that MODE achieved the lowest average objective functions values for T_S, C_m and GHG_m. MODE had the lowest coefficient of variation for all objective functions. On the other hand, MOJAYA had the highest coefficient of variation for T_S, and MOPSO had the highest coefficient of variation for C_m and GHG_m. MODE provided the largest hypervolume indicator (81.721%) followed by MOSFL while MODA provided the least hypervolume indicator (20.112%). In terms of the generational distance, MODE achieved the smallest generational distance (0.029). Nevertheless, MOJAYA attained the largest generational distance (5.482). With respect to the spacing metric, MODE attained the lowest spacing (0.1881) while MOJAYA attained the highest spacing (157.4636). MODE attained the smallest diversity (0.5229) while MODA attained the largest diversity (1.5615). For the spread, MODE achieved the highest value (0.9618). Nevertheless, MOPSO yielded the least value (0.4394). MODE achieved the lowest values of coverage (0.4087) while MOGWO provided the highest value (0.9997). Genetic algorithm is considered as the most commonly-utilized meta-heuristic in resource allocation problems. In this context, the average values of T_S, C_m and GHG_m achieved by MOGA are 105.382, 904.482 and 16.447, respectively. As such, compared to the MOGA the developed MODE accomplished an improvement in the reduction of time, cost and greenhouse by 71.01%, 27.87% and 39.29%, respectively. In the view of the afore-comparisons, it can be inferred that the proposed MODE outperformed other meta-heuristic optimization algorithms with respect to the accuracy, diversity and cardinality performance indicators.

INSERT TABLE 11

In order to elaborate more about the performance of the meta-heuristic optimization algorithms, the box plots based on the diversity metric and generational distance of them are presented in Figures 12.a and 12.b, respectively. The box plots enable assessment of robustness of the different meta-heuristics through mapping the distribution and skewness of the numerical data. It displays the minimum, first quartile, third quartile and maximum values of the multiple runs. The solid line in the box encodes the second quartile or the median value. The height of the box (space between the first and third quartiles) delineates the robustness of the algorithm, which is one of the main aspects to judge the performance of meta-heuristics. Lower spread in the box plot signifies more robustness performance of the model. By comparing the box plots, it can be observed that MODE provides more stable and consistent results while MOJAYA and MOGA yielded unsteady performances. Figures 12.a and 12.b also demonstrate that MODE sustains significant lower diversity and generational distance with respect to other algorithms over the course of the different runs. As such, MODE provides superior and more robust performance in comparison to the state of art meta-heuristics. Wilcoxn test, Mann-Whitney-U test, Kruskal–Wallis test, binomial sign test, and Mood's median test of the multi-objective optimization models are shown in Table 12. As can be seen, $P-$ values of the pairs (MODE, MOGA), (MODE, MOPSO), (MODE, MODA), (MODE, MOGWO), (MODE, MOJAYA) and (MODE, MOSFL) are less than 0.05. This evinces that there are significant differences in the search capacities of the proposed multi-objective optimization model with respect to the state of art meta heuristics.

INSERT FIGURE 12

INSERT TABLE 12

The multi-criteria decision making model is employed to select the best solution among the Pareto optimal resource allocation plans obtained from the multi-objective optimization model. It constitutes three attributes, namely T_S, C_m and GHG_m, whereas the weights of the attributes are calculated based on the Shannon entropy method. The calculations of the weights of the attributes are presented in Table 13. As shown in Table 13, the weights of T_S, C_m and GHG_m are 44.588%, 27.102% and 28.31%, respectively. PROMETHEE II is employed to generate a full ranking of the resource allocation plans. The preference threshold values of T_S, C_m and GHG_m are equal to 73.51, 490.134 and 8.058, respectively. A sample of the solution ranking obtained from the PROMETHEE II is depicted in Table 14. The best solution is the one which provides the highest net flow. As can be seen, the solution [5, 1, 5, 4, 10, 7, 10, 5, 5, 8, 10, 6, 5, 1] is selected as the best solution. It yields T_S, C_m and GHG_m of 29.742, 652.918 and 9.719, respectively and a net flow $ø(a)$ of 0.2213. Furthermore, this solution achieved UNI_{AVG_UTIL} and UNI_{STD_UTIL} of 95.133% and 9.533%, respectively. This demonstrates that the developed resource allocation method is capable of minimizing time, cost and greenhouse gases while accommodating the uniformity in the utilization of resources.

The solution [5, 2, 5, 4, 6, 7, 7, 1, 4, 9, 7, 4, 4, 5] achieved the fourteenth rank such that, it attained T_S, C_m and GHG_m of 30.469, 652.567 and 10.208, respectively and a net flow $ø(a)$ of 0.2123. It is expected that the developed integrative evolutionary-based method can provide an efficient multi-objective optimization platform that aids decision-makers to allocate limited resources efficiently through integrating different alternatives and activities in a comprehensive paradigm that the enables the fulfilment of targeted objectives and satisfaction of project constraints. It can be also used by the contractors when planning for the resources needed for the bridge deck replacement in an attempt to minimize time, cost and environmental emissions while

accommodating the efficiency and uniformity in the utilization of resources. Additionally, it can serve as a template to be used by construction firms in other different construction operations for the purpose of accomplishing better utilization of resources and for minimizing their duration, cost and environmental impact in the delivery of their projects.

INSERT TABLE 13

INSERT TABLE 14

CONCLUSION

The number of deteriorating bridges is increasing dramatically, and the presence of limited funding for repairing and replacing the degraded bridges stand as a significant challenge that is further complicated by the increase in construction costs. As such, bridge management systems are developed to aid decision makers in maximizing the safety, functionality and serviceability of bridge networks while maintaining cost-effective repair, rehabilitation and replacement plans within available budget. The present study introduces an automated integrative evolutionary-based platform to simulate and optimize performance aspects and utilization rate of resource allocation plans in bridge deck replacement projects. It houses three models namely, discrete event simulation, machine learning and multi-objective optimization. STROBOSCOPE simulation engine is adopted to model the bridge deck replacement process. A novel surrogate machine learning model is then developed to build an efficient prediction model that can alleviate the shortcomings of timely and computationally expensive simulation. The data-driven surrogate machine learning model is established for the purpose of emulating automatically the performance aspects of time, cost, greenhouse gases and utilization rates for the different resource allocation plans. In it, invasive weed optimization algorithm is utilized to train the Elman neural network to overcome the drawbacks of the gradient descent algorithm,

such that a variable-length optimization model is designed for the purpose of parameter and structural learning of the Elman neural network. The third tier involves a multi-objective differential evolution model to identify the optimum number of resources according to minimizing the project duration, cost and greenhouse gases, and subject to the utilization rates of the resources and their dispersion.

The validation of the surrogate machine learning model is envisioned on three stages. In the first stage, results declared that there are no statistical significant difference between the machine learning model and discrete event simulation model based on Mann-Whitney-U test. In the second stage, the developed model was compared with nine state of art prediction models reported for their high recognition capacities namely, back-propagation artificial neural network, radial basis neural network, generalized regression neural network, convolutional neural network, linear kernel support vector machines, radial kernel support vector machines, gradient boosted decision trees, Gaussian process and K-nearest neighbors. It outperformed the previously-mentioned regression models as per several performance diagnostics. For instance, $\mathrm{ENN-IWO}$ attained MAPE, MAE and RMSE of 4.873%, 78.466 and 39.515, respectively in cost prediction based on split validation. In third stage, the proposed $\mathrm{ENN-IWO}$ demonstrated significant superior performance exemplified through a set of non-parametric tests.

The developed multi-objective optimization model is validated through comparisons against a set of well-performing meta-heuristics namely, genetic algorithm, particle swarm optimization algorithm, dragonfly algorithm, grey wolf optimization algorithm, Jaya algorithm and shuffled frog-leaping algorithm and non-linear programming. It significantly outperformed them such that, it achieved hypervolume indicator, generational distance, spacing, diversity, spread and coverage of 81.721%, 0.029, 0.1881, 0.5229, 0.9618 and 0.4087, respectively. Additionally, the

developed optimization model accomplished an improvement in the reduction of time, cost and greenhouse gases by 71.01%, 27.87% and 39.29%, respectively when compared against the commonly-used genetic algorithm. PROMETHEE II is then applied to select the best alternative among the set of Pareto optimal solutions. Results clearly demonstrated the efficiency of the developed method in modeling the bridge deck replacement, simulating the performance aspects and utilization rates of resource allocation plans, and optimal allocation of resources while satisfying the pre-defined constraints. As such, the developed integrative evolutionary-based method can be deployed as an efficient mechanism that enables decision makers to design cost-effective and sustainable resource allocation plans meanwhile ensuring the efficient utilization of their resources.

Data Availability Statement

Some or all data, models or code that support the findings of this study are available from the corresponding author upon request.

REFERENCES

1. AASHTO Highways subcommittee on Bridges and Structures. (2011). *The Manual for Bridge Evaluation, Second Edition*. Washington, D.C, United States.
2. Ali, M. S., Aslam, M. S., & Mirza, M. S. (2016). "A sustainability assessment framework for bridges – a case study: Victoria and Champlain Bridges, Montreal." *Structure and Infrastructure Engineering*, *12*(11), 1381–1394.
3. Al-Sudani, A. Z., Salih, S. Q., sharafati, A., & Yaseen, Z. M. (2019). "Development of multivariate adaptive regression spline integrated with differential evolution model for streamflow simulation." *Journal of Hydrology*, *573*, 1–12.

4. AlSukker, A., Khushaba, R. N., and Al-Ani, A. (2010). “Enhancing the diversity of genetic algorithm for improved feature selection.” *IEEE International Conference on Systems, Man and Cybernetics*, Istanbul, 1325–1331.
5. Amini, A., Nikraz, N., and Fathizadeh, A. (2016). “Identifying and evaluating the effective parameters in prioritization of urban roadway bridges for maintenance operations”. *Australian Journal of Civil Engineering*, 14(1), 23-34.
6. Azizipour, M., Ghalenoei, V., Afshar, M. H., & Solis, S. S. (2016). “Optimal Operation of Hydropower Reservoir Systems Using Weed Optimization Algorithm.” *Water Resources Management*, *30*(11), 3995–4009.
7. Babaee Tirkolaee, E., Goli, A., Pahlevan, M., & Malekalipour Kordestanizadeh, R. (2019). “A robust bi-objective multi-trip periodic capacitated arc routing problem for urban waste collection using a multi-objective invasive weed optimization.” *Waste Management and Research*, *37*(11), 1089–1101.
8. Badawy, A. M. (2017). “*Assessment of Bridges’ Expansion Joints In Egypt*.” M.Sc. thesis, American University in Cairo, Egypt.
9. Bagloee, S. A., & Sarvi, M. (2018). “An outer approximation method for the road network design problem.” *PLoS ONE*, *13*(3), 1–28.
10. Brankovic, J. M., Markovic, M., & Nikolic, D. (2018). “Comparative study of hydraulic structures alternatives using promethee II complete ranking method.” *Water Resources Management*, *32*(10), 3457–3471.
11. Brans, J. P., Vincke, P., & Mareschal, B. (1986). “How to select and how to rank projects : The PROMETHEE method.” *European Journal of Operational Research*, *24*, 228–238.
12. Brans, J. P., & Vincke, D. P. (1985). “A Preference Ranking Organisation Method: (The

PROMETHEE Method for Multiple Criteria Decision-Making).” *Management Science*, *31*(6), 647–656.

13. Bukhsh, Z. A., Stipanovic, I., & Doree, A. G. (2020). “Multi-year maintenance planning framework using multi-attribute utility theory and genetic algorithms.” *European Transport Research Review*, *12*(3), 1–13.
14. Bukhsh, Z. A., Stipanovic, I., Klanker, G., Connor, A. O., & Doree, A. G. (2019). “Network level bridges maintenance planning using Multi-Attribute Utility Theory.” *Structure and Infrastructure Engineering*, *15*(7), 872–885.
15. Caterpillar Inc. (2013). Caterpillar Performance Handbook, Illinois, United States of America.
16. Chai, J., Huang, P., & Sun, Y. (2020). “Differential evolution - based system design optimization for net zero energy buildings under climate change.” *Sustainable Cities and Society*, *55*, 1-14.
17. Chen, Y. W., Cheng, C. Y., Li, S. F., & Yu, C. H. (2018). “Location optimization for multiple types of charging stations for electric scooters.” *Applied Soft Computing*, *67*, 519–528.
18. Chen, X., Wang, W., Xie, G., Hontecillas, R., Verma, M., Leber, A., Bassaganya-Riera, A., Abedi, V. (2019). “Multi-Resolution Sensitivity Analysis of Model of Immune Response to Helicobacter pylori Infection via Spatio-Temporal Metamodeling.” *Frontiers in Applied Mathematics and Statistics*, *5*, 1-15.
19. Contreras-nieto, C., Shan, Y., Lewis, P., & Ann, J. (2019). “Bridge maintenance prioritization using analytic hierarchy process and fusion tables.” *Automation in Construction*, *101*, 99–110.

20. Cui, Z., Zhang, J., Wu, D., Cai, X., Wang, H., Zhang, W., & Chen, J. (2020). "Hybrid many-objective particle swarm optimization algorithm for green coal production problem." *Information Sciences, 518,* 256–271.
21. Dindarloo, S. R., & Siami-Irdemoosa, E. (2016). "Determinants of fuel consumption in mining trucks." *Energy*, *9*(10), 232–240.
22. Falahiazar, L., & Shah-Hosseini, H. (2018). "Optimisation of engineering system using a novel search algorithm: the Spacing Multi-Objective Genetic Algorithm." *Connection Science*, *30*(3), 326–342.
23. Farzam, A., Nollet, M.-J., & Khaled, A. (2016). "Integration of site conditions information using geographic information system for the seismic evaluation of bridges." *Canadian Society of Civil Engineering Annual Conference: Resilient Infrastructure*, London,Canada, 1-4 June, 1-10.
24. Fayaz, M., Shah, H., Aseere, A., Mashwani, W., & Shah, A. (2019). "A Framework for Prediction of Household Energy Consumption Using Feed Forward Back Propagation Neural Network." *Technologies*, *7*(2), 1-16.
25. Felio, G. (2016). "*Canadian Infrastructure Report Card"*. Canadian Construction Association, Canadian Public Works Association, Canadian Society for Civil Engineering, and Federation of Canadian Municipalities, Canada. <www.canadainfrastructure.ca/downloads/Canadian_Infrastructure_Report_2016.pdf> (06.05.2016).
26. Flower, D.J.M., & Sanjayan, J.G. (2007). "Green house gas emissions due to concrete manufacture." *The International Journal of Life Cycle Assessment*. 12, 282–288.

27. García de Soto, B., Agustí-Juan, I., Hunhevicz, J., Joss, S., Graser, K., Habert, G., & Adey, B. T. (2018). "Productivity of digital fabrication in construction: Cost and time analysis of a robotically built wall." *Automation in Construction, 92,* 297–311.
28. Gervásio, H., & Simões Da Silva, L. (2012). "A probabilistic decision-making approach for the sustainable assessment of infrastructures." *Expert Systems with Applications, 39*(8), 7121–7131.
29. Gordian RSMeans Data. (2017). Building Construction Cost Data with rsmeans data.
30. Hafezalkotob, A., & Hafezalkotob, A. (2015). "Extended MULTIMOORA method based on Shannon entropy weight for materials selection." *Journal of Industrial Engineering International, 12*(1), 1–13.
31. Hamza, F., Abderazek, H., Lakhdar, S., Ferhat, D., Yildiz, A. R. (2018). "Optimum design of cam-roller follower mechanism using a new evolutionary algorithm." *The International Journal of Advanced Manufacturing Technology, 99*:1267–1282.
32. Hansen, S., & Sadeghian, P. (2020). "Recycled gypsum powder from waste drywalls combined with fly ash for partial cement replacement in concrete." *Journal of Cleaner Production, 274.*
33. Hasan, U., Whyte, A., & Al Jassmi, H. (2020). "Life cycle assessment of roadworks in United Arab Emirates: Recycled construction waste, reclaimed asphalt pavement, warm-mix asphalt and blast furnace slag use against traditional approach." *Journal of Cleaner Production, 257*, 1-16.
34. Inyim, P., Zhu, Y., & Orabi, W. (2016). "Analysis of Time, Cost, and Environmental Impact Relationships at the Building-Material Level." *Journal of Management in Engineering, 32*(4), 1-12.

35. Jabin, S. (2014). “Stock market prediction by using artificial neural network.” *International Journal of Computer Applications, 99*(9), 718–722.
36. Jahan, A., Mustapha, F., Sapuan, S. M., Ismail, M. Y., & Bahraminasab, M. (2012). “A framework for weighting of criteria in ranking stage of material selection process.” *International Journal of Advanced Manufacturing Technology, 58*, 411–420.
37. Jaskowski, P., & Biruk, S. (2020). “Scheduling of Repetitive Construction Processes With Concurrent Work of Similarly Specialized Crews.” *Journal of Civil Engineering and Management, 26*(6), 579–589.
38. Jassim, H. S. H., Lu, W., & Olofsson, T. (2016). A practical method for assessing the energy consumption and CO2 emissions of mass haulers. *Energies, 9*(10), 1-16.
39. Jin, C. (2011). “Software reliability prediction based on support vector regression using a hybrid genetic algorithm and simulated annealing algorithm.” *IET Software, 5*(4), 398–405.
40. Kamal, M., & Inel, M. (2019). “Optimum Design of Reinforced Concrete Continuous Foundation Using Differential Evolution Algorithm.” *Arabian Journal for Science and Engineering, 44*(10), 8401–8415.
41. Khetwal, A., Rostami, J., & Nelson, P. P. (2020). “Investigating the impact of TBM downtimes on utilization factor based on sensitivity analysis.” *Tunnelling and Underground Space Technology, 106,* 1-13.
42. Kim, H., Bang, S., Jeong, H., Ham, Y., & Kim, H. (2018). “Analyzing context and productivity of tunnel earthmoving processes using imaging and simulation.” *Automation in Construction, 92,* 188–198.
43. Kim, N., Moawad, A., Vijayagopal, R., & Rousseau, A. (2016). “Impact of Fuel Cell and Storage System Improvement on Fuel Consumption and Cost.” *World Electric Vehicle*

Journal, *8*, 305–314.

44. Köker, R. (2013). “A Genetic Algorithm Approach to a Neural-network-based Inverse Kinematics Solution of Robotic Manipulators Based on Error Minimization.” *Information and Control*, 222, 528–543.
45. Kolios, A., Mytilinou, V., & Lozano-minguez, E. (2016). “A Comparative Study of Multiple-Criteria Decision-Making Methods under Stochastic Inputs.” *Energies*, *9*(7), 1–21.
46. Le, D. T., Bui, D. K., Ngo, T. D., Nguyen, Q. H., and Nguyen-Xuan, H. (2019). “A novel hybrid method combining electromagnetism-like mechanism and firefly algorithms for constrained design optimization of discrete truss structures.” *Computers and Structures*, *212*, 20–42.
47. Le, T., Vo, M. T., Vo, B., Hwang, E., Rho, S., & Baik, S. W. (2019). “Improving Electric Energy Consumption Prediction Using CNN and Bi-LSTM. ” *Applied Sciences*, *9*(20), 1–12.
48. Lee, D.-E., Lim, T.-K., & Arditi, D. (2012). “Stochastic Project Financing Analysis System for Construction.” *Journal of Construction Engineering and Management*, *138*(3), 376–389.
49. Lewis, P., & Hajji, A. (2012). “Estimating the economic, energy, and environmental impact of earthwork activities.” *Construction Research Congress 2012: Construction Challenges in a Flat World*, Indiana, 1770–1779.
50. Limsawasd, C., & Athigakunagorn, N. (2017). “Optimizing Construction productivity and resources in building projects under uncertainty.” *6th CSCE-CRC International Construction Specialty Conference jointly with Canadian Society for Civil Engineering Annual Conference*, 1120–1129.
51. Mahdi, I. M., Khalil, A. H., Mahdi, H. A., & Dina, M. M. (2019). “Decision support system for optimal bridge ’ maintenance.” *International Journal of Construction Management*, 1–15.

52. Mahmoodian, M., Torres-matallana, J. A., Leopold, U., Schutz, G., & Clemens, F. H. L. R. (2018). "A Data-Driven Surrogate Modelling Approach for Acceleration of Short-Term Simulations of a Dynamic Urban Drainage Simulator." *Water*, *10*(12), 1–17.
53. Makan, A., & Fadili, A. (2020). "Sustainability assessment of large-scale composting technologies using PROMETHEE method." *Journal of Cleaner Production*, *261*, 121244, 1-8.
54. Mao, X., Jiang, X., Yuan, C., & Zhou, J. (2020). "Modeling the Optimal Maintenance Scheduling Strategy for Bridge Networks." *Applied Sciences*, *10*(2), 1–16.
55. Markiz, N., & Jrade, A. (2018). "Integrating Fuzzy-Logic Decision Support With A Bridge Information Management System (BRIMS) at The Conceptual Stage Of Bridge Design." *Journal of Information Technology in Construction*, *23*, 92–121.
56. Martinez, J. C. (1996). "*STROBOSCOPE State and Resource Based Simulation of Construction Processes*. "PhD. thesis, University of Michigan, United States of America.
57. Marzouk, M., & Younes, A. (2013). "A Simulation Based Decision Tool for Transportation of Ready Mixed Concrete." *International Journal of Architecture, Engineering and Construction*, *2*(4), 234–245.
58. Miyamoto, A., Kawamura, K., & Nakamura, H. (2001). "Development of a bridge management system for existing bridges." *Advances in Engineering Software*, *32*, 821–833.
59. Mohammed Abdelkader, E., Moselhi, O., Marzouk, M. & Zayed, T. (2020). "A Multi-objective Invasive Weed Optimization Method for Segmentation of Distress Images." *Intelligent automation and soft computing*, *26*(4), 643-661.
60. Nurdin, A., Kristiawan, S. A., & Handayani, D. (2017). "Determination of the bridge maintenance and rehabilitation priority scale in kabupaten Pinrang. " *Journal of Physics:*

Conference Series, *795*, 1–7.

61. Osman, H., Ammar, M., & El-Said, M. (2017). “Optimal scheduling of water network repair crews considering multiple objectives.” *Journal of Civil Engineering and Management*, *23*(1), 28–36.
62. Ozcan-Deniz, G., & Zhu, Y. (2015). “A multi-objective decision-support model for selecting environmentally conscious highway construction methods.” *Journal of Civil Engineering and Management*, *21*(6), 733–747.
63. Parnianifard, A., Azfanizam, A. S., Ariffin, M. K. A., Ismail, M. I. S., & Ale Ebrahim, N. (2019). “Recent developments in metamodel based robust black-box simulation optimization: An overview.” *Decision Science Letters*, *8*(1), 17–44.
64. Petroodi, S. E. H., Dit Eynaud, A. B., Klement, N., and Tavakkoli-Moghaddam, R. (2019). “Simulation-based optimization approach with scenario-based product sequence in a reconfigurable manufacturing system (RMS): A case study.” *IFAC-PapersOnLine*, *52*(13), 2638–2643.
65. Podolski, M., & Sroka, B. (2019). “Cost optimization of multiunit construction projects using linear programming and metaheuristic-based simulated annealing algorithm.” *Journal of Civil Engineering and Management*, *25*(8), 848–857.
66. Poonthalir, G., & Nadarajan, R. (2018). “A Fuel Efficient Green Vehicle Routing Problem with varying speed constraint (F-GVRP).” *Expert Systems with Applications*, *100*, 131–144.
67. Prabha, D. R., Jayabarathi, T., Mageshvaran, R., Bharadwaj, V. R., & Siddhartha, G. (2016). “Invasive weed optimization for economic dispatch with valve point effects.” *Journal of Engineering Science and Technology*, *11*(2), 237–251.
68. Puri, V., & Martinez, J. C. (2013). "Modeling of Simultaneously Continuous and Stochastic

Construction Activities for Simulation." *Journal of Construction Engineering and Management, 139*(8), 1037–1045.

69. Rashidi, M., Ghodrat, M., Samali, B., Kendall, B., & Zhang, C. (2017). "Remedial Modelling of Steel Bridges through Application of Analytical Hierarchy Process (AHP). " *Applied Sciences, 7*(2), 1–20.
70. Rojob, H., & El-Hacha, R. (2018). "Fatigue performance of RC beams strengthened with self-prestressed iron-based shape memory alloys." *Engineering Structures, 168,* 35–43.
71. Safa, M., Shahi, A., Haas, C. T., & Hipel, K. W. (2014). "Supplier selection process in an integrated construction materials management model." *Automation in Construction, 48,* 64–73.
72. Saravanan, B., Vasudevan, E. R., & Kothari, D. P. (2014). "Unit commitment problem solution using invasive weed optimization algorithm." *International Journal of Electrical Power and Energy Systems, 55,* 21–28.
73. Sennah, K., Juette, B., Witt, C., & Combar, P. M. (2011). "Vehicle Crash Testing On a GFRP-Reinforced PL-3 Concrete Bridge Barrier." *Proceedings of the 4th International Conference on Durability and Sustainability of Fibre Reinforced Polymer Composites for Construction and Rehabilitation,* Québec City, Canada, 20-22 July, 1–8.
74. Seo, J., Lee, S., & Seo, J. (2016). Simulation-Based Assessment of Workers' Muscle Fatigue and Its Impact on Construction Operations. *Journal of Construction Engineering and Management, 142*(11), 1-12.
75. Seyedpoor, S. M., Shahbandeh, S., & Yazdanpanah, O. (2015). "An efficient method for structural damage detection using a differential evolution algorithm-based optimisation approach." Civil Engineering and Environmental Systems, *32*(3), 230-250.

76. Shehwaro, H., Zankoul, E., & Khoury, H. (2016). An Agent-Based Approach for Modeling the Effect of Learning Curve on Labor Productivity Bridges. *Proceedings of the First European and Mediterranean Structural Engineering and Construction*, Istanbul, 1-6.
77. Shim, H. S., and Lee, S. H. (2017). "Balanced Allocation of Bridge Deck Maintenance Budget Through." *KSCE Journal of Civil Engineering*, *21*(4), 1039-1046.
78. Shreyas, S. K., and Dey, A. (2019). "Application of soft computing techniques in tunnelling and underground excavations: state of the art and future prospects." *Innovative Infrastructure Solutions*, *4*(1), 1-15.
79. Song, J., Yang, Y., Wu, J., Wu, J., Sun, X., & Lin, J. (2018). "Adaptive surrogate model based multiobjective optimization for coastal aquifer management." *Journal of Hydrology*, *561*, 98–111.
80. Statistics Canada. (2009). "*Age of Public Infrastructure: A Provincial Perspective*". < http://www.statcan.gc.ca/pub/11-621-m/11-621-m2008067-eng.htm> (20.12.2016).
81. Storn, R., & Price, K. (1997). "Differential Evolution - A simple and efficient adaptive scheme for global optimization over continuous spaces. " *Journal of Global Optimization*, *11*(4),341-359.
82. Su, L., Trivedi, R., Sapra, N. V., Piggott, A. Y., Vercruysse, D., and Vučković, J. V. (2018). "Fully-automated optimization of grating couplers." *Optics Express*, *26*(4), 4766.
83. Tesfamariam, S., Bastidas-Arteaga, E., & Lounis, Z. (2018). "Seismic retrofit screening of existing highway bridges with consideration of chloride-induced deterioration: A bayesian belief network model." *Frontiers in Built Environment*, *4*, 1–11.

84. Thipparat, T. (2013). “Integration between neuro-fuzzy system and Monte Carlo simulation for duration estimation of the bored piles.” *International Journal of Business and Systems Research, 7*(2), 189–207.
85. Tomczak, M., & Jaśkowski, P. (2020). “New Approach to Improve General Contractor Crew’s Work Continuity in Repetitive Construction Projects.” *Journal of Construction Engineering and Management, 146*(5), 1–11.
86. Vand, M., & Xavier, A. S. (2017). “Modeling of resource-driven scheduling in high- rise buildings using genetic algorithm.” *International Journal of Advances in Engineering & Technology*, *10*(2), 185–191.
87. Viami International Inc. and the Technology Strategies Group. (2013). “*Market Study for Aluminium Use in Roadway Bridges”*, Montreal, Canada.
88. Vulević, T., & Dragović, N. (2017). “Multi-criteria decision analysis for sub-watersheds ranking via the PROMETHEE method.” *International Soil and Water Conservation Research, 5*(1), 50–55.
89. Wang, J., Zhang, W., Li, Y., Wang, J., and Zhangli Dang. (2014). “Forecasting Wind Speed Using Empirical Mode Decomposition and Elman Neural Network.” *Applied Soft Computing*, 23, 452–459.
90. Wu, D., Yuan, C., Kumfer, W., & Liu, H. (2017). “A Life-cycle Optimization Model using Semi-markov Process for Highway Bridge Maintenance.” *Applied Mathematical Modelling,* 43, 45–60.
91. Wu, X., & Hu, F. (2020). “Analysis of ecological carrying capacity using a fuzzy comprehensive evaluation method.” *Ecological Indicators, 113,* 1–13.
92. Wu, Y., Zhang, B., Wu, C., Zhang, T., & Liu, F. (2019). “Optimal site selection for parabolic

trough concentrating solar power plant using extended PROMETHEE method: A case in China." *Renewable Energy, 143*, 1910–1927.

93. Yahya, A. S. A., Ahmed, A. N., Othman, F. B., Ibrahim, R. K., Afan, H. A., El-Shafie, A., Fai, C. B., Hossain, F. B., Ehteram, M., & Elshafie, A. (2019). "Water quality prediction model based support vector machine model for ungauged river catchment under dual scenarios." *Water, 11*(6), 1-16.
94. Yagiz, S., Yazitova, A., & Karahan, H. (2020). "Application of differential evolution algorithm and comparing its performance with literature to predict rock brittleness for excavatability. " *International Journal of Mining, Reclamation and Environment*, 1–14.
95. Yi, C. Y., Gwak, H. S., & Lee, D. E. (2017). "Stochastic carbon emission estimation method for construction operation." *Journal of Civil Engineering and Management*, *23*(1), 137–149.
96. Yoon, Y., & Hastak, M. (2017). "Condition Improvement Measurement Using the Condition Evaluation Criteria of Concrete Bridge Decks." *Journal of Transportation Engineering*, *142*(11), 1–8.
97. Yossyafra, Angelia, N., Yosritzal, Meyadtri, & Mazni5, D. I. (2019). "Determining the priority criteria and ranking of provincial bridge maintenance in West Sumatra using a combination of the Fuzzy Analytical Hierarchy Process and VIKOR-Modification methods." *IOP Conference Series: Materials Science and Engineering.* 602**,** 8-9 November**,** Padang, Indonesia**,** 1-9.
98. Younes, T., Ni, F. M., & Tighe, S. (2020). "Risk analysis in paving operations using discrete event simulation : a case study of Taiwan permeable asphalt concrete pavement pilot road project. " *International Journal of Pavement Engineering*, *21*(7), 830-740.

99. Yu, X., Yu, X., Lu, Y., & Sheng, J. (2018). “Economic and Emission Dispatch Using Ensemble Multi-Objective Differential Evolution Algorithm. ” *Sustainability*, *10*(2), 1–17.

100. Yun, S., Cho, H., Tae, Y., Ahn, B., An, S. H., & Huh, Y. (2012). “Productivity analysis of steel works for cost estimation of public projects in Korea.” *KSCE Journal of Civil Engineering*, *16*(1), 1–7.

101. Zankoul, E., Khoury, H., & Awwad, R. (2015). “Evaluation of agent-based and discrete-event simulation for modeling construction earthmoving operations.” *32nd International Symposium on Automation and Robotics in Construction*, Finland, 1-8.

102. Zhang, C., Zayed, T., & Hammad, A. (2008). “Resource Management of Bridge Deck Rehabilitation: Jacques Cartier Bridge Case Study.” *Journal f Construction Engineering and Management*, *134*(5), 311–319.

103. Zhang, H. (2015). “Simulation-Based Estimation of Fuel Consumption and Emissions of Asphalt Paving Operations.” *Journal of Computing in Civil Engineering*, *29*(2), 1-13.

104. Zhang, J., Li, Y., Xiao, W., & Zhang, Z. (2020). “Non-iterative and Fast Deep Learning: Multilayer Extreme Learning Machines.”*Journal of the Franklin Institute*, 1-31.

105. Zou, X., Zhang, L., & Zhang, Q. (2018). “A Biobjective Optimization Model for Deadline Satisfaction in Line-of-Balance Scheduling with Work Interruptions Consideration.” *Mathematical Problems in Engineering*, *2018*, Article ID 6534021, 12 pages.

List of Figures

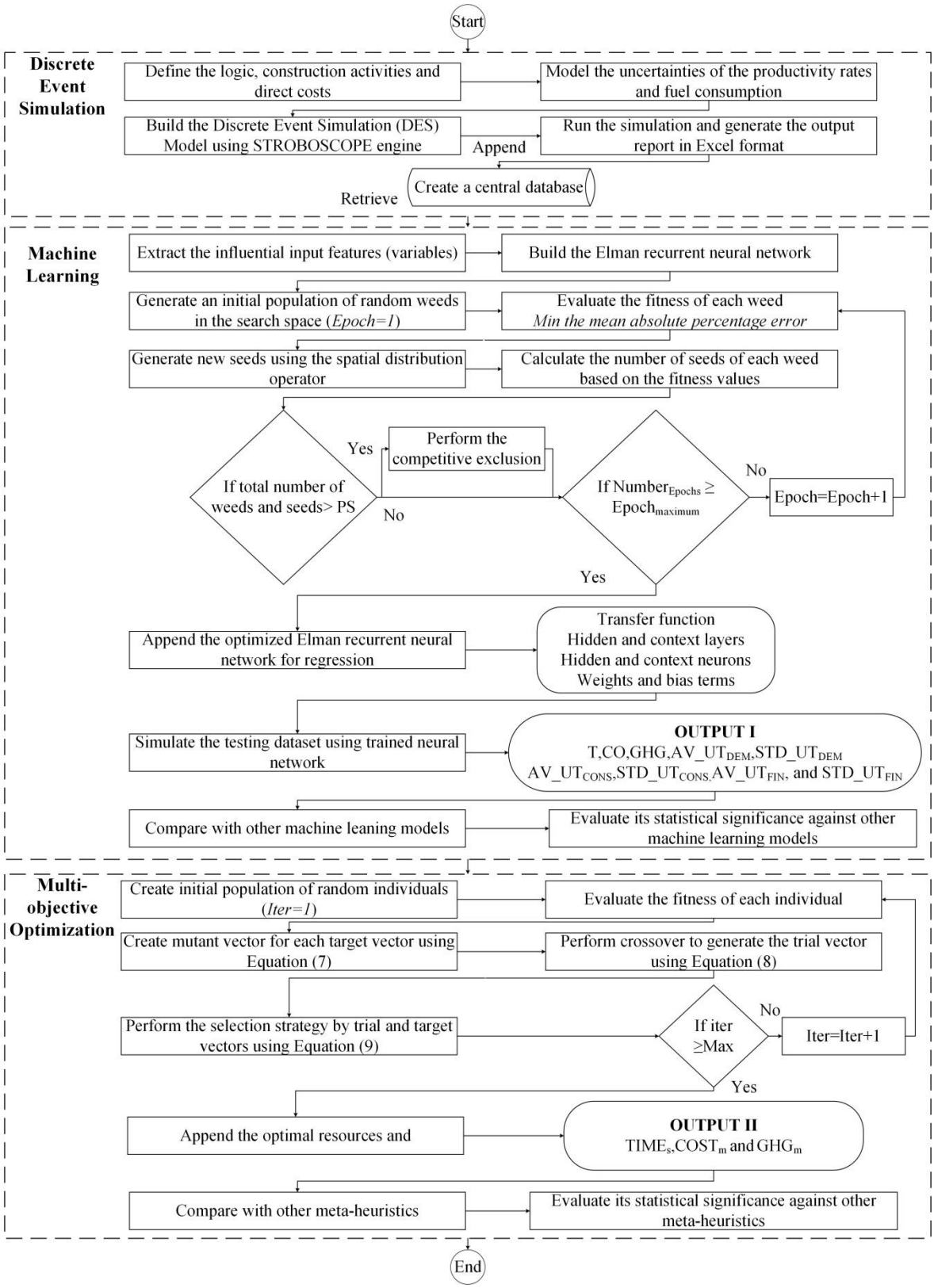
Start
Discrete Event Simulation
Define the logic, construction activities and direct costs
Model the uncertainties of the productivity rates and fuel consumption
Build the Discrete Event Simulation (DES) Model using STROBOSCOPE engine
Append
Run the simulation and generate the output report in Excel format
Retrieve
Create a central database
Machine Learning
Extract the influential input features (variables)
Build the Elman recurrent neural network
Generate an initial population of random weeds in the search space (Epoch=1)
Evaluate the fitness of each weed
Min the mean absolute percentage error
Generate new seeds using the spatial distribution operator
Calculate the number of seeds of each weed based on the fitness values
If total number of weeds and seeds> PS
Yes
Perform the competitive exclusion
No
If Number Epochs ≥ Epoch maximum
No
Epoch=Epoch+1
Yes
Append the optimized Elman recurrent neural network for regression
Transfer function
Hidden and context layers
Hidden and context neurons
Weights and bias terms
Simulate the testing dataset using trained neural network
OUTPUT I
T,CO,GHG,AV_UT DEM,STD_UT DEM
AV_UT CONS,STD_UT CONS,AV_UT FIN, and STD_UT FIN
Compare with other machine leaning models
Evaluate its statistical significance against other machine learning models
Multi-objective Optimization
Create initial population of random individuals (Iter=1)
Evaluate the fitness of each individual
Create mutant vector for each target vector using Equation (7)
Perform crossover to generate the trial vector using Equation (8)
Perform the selection strategy by trial and target vectors using Equation (9)
If iter ≥Max
No
Iter=Iter+1
Yes
Append the optimal resources and
OUTPUT II
TIME s,COST m and GHG m
Compare with other meta-heuristics
Evaluate its statistical significance against other meta-heuristics
End

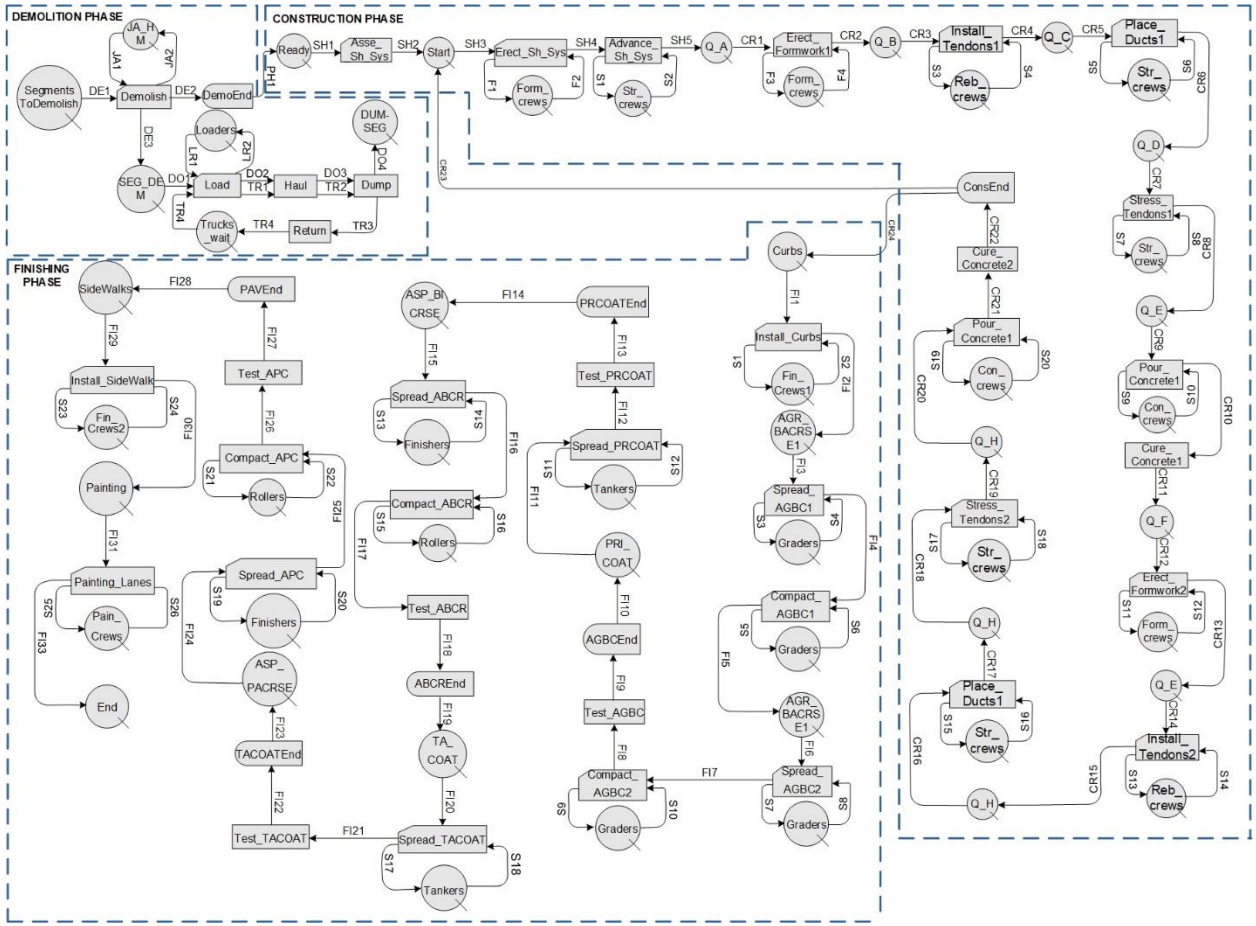
DEMOLITION PHASE
CONSTRUCTION PHASE
FINISHING PHASE
JA_HM
JA1
JA2
Segments ToDemolish
DE1
Demolish
DE2
DemoEnd
PH1
DE3
Loaders
LR1
LR2
SEG_DEM
DO
Load
DO2
TR1
Haul
DO3
TR2
Dump
DO4
DUM-SEG
TR4
Trucks_wait
TR4
Return
TR3
Ready
SH1
Asse_Sh_Sys
SH2
Start
SH3
Erect_Sh_Sys
SH4
Advance_Sh_Sys
SH5
F1
Form_crews
F2
S1
Str_crews
S2
Q_A
CR1
Erect_Formwork1
CR2
F3
Form_crews
F4
Q_B
CR3
Install_Tendons1
CR4
S3
Reb_crews
S4
Q_C
CR5
Place_Ducts1
S5
Str_crews
S6
CR6
Q_D
CR7
Stress_Tendons1
S7
Str_crews
S8
CR8
Q_E
CR9
Pour_Concrete1
S9
Con_crews
S10
CR10
Cure_Concrete1
CR11
Q_F
CR12
Erect_Formwork2
S11
Form_crews
S12
CR13
Q_E
CR14
Install_Tendons2
S13
Reb_crews
S14
CR15
Q_H
CR16
Place_Ducts1
S15
Str_crews
S16
CR17
Q_H
CR18
Stress_Tendons2
S17
Str_crews
S18
CR19
Q_H
CR20
Pour_Concrete1
S19
Con_crews
S20
CR21
Cure_Concrete2
CR22
ConsEnd
CR23
Curbs
CR24
FI1
Install_Curbs
S1
Fin_Crews1
S2
F2
AGR_BACRSE1
FI3
Spread_AGBC1
S3
Graders
S4
F4
Compact_AGBC1
S5
Graders
S6
F5
AGR_BACRSE1
FI6
Spread_AGBC2
S7
Graders
S8
FI7
Compact_AGBC2
S9
Graders
S10
FI8
Test_AGBC
FI9
AGBCEnd
FI10
PRI_COAT
FI11
S11
Tankers
S12
FI12
Spread_PRCOAT
Test_PRCOAT
FI13
PRCOATEnd
FI14
ASP_BCRSE
FI15
Spread_ABCR
S13
Finishers
S14
FI16
Compact_ABCR
S15
Rollers
S16
FI17
Test_ABCR
FI18
ABCREnd
FI19
TA_COAT
FI20
Spread_TACOAT
S17
Tankers
S18
FI21
Test_TACOAT
FI22
TACOATEnd
FI23
ASP_PACRSE
FI24
Spread_APC
S19
Finishers
S20
FI25
Compact_APC
S21
Rollers
S22
FI26
Test_APC
FI27
PAVEnd
FI28
SideWalks
FI29
Install_SideWalk
S23
Fin_Crews2
S24
FI30
Painting
FI31
Painting_Lanes
S25
Pain_Crews
S26
FI33
End

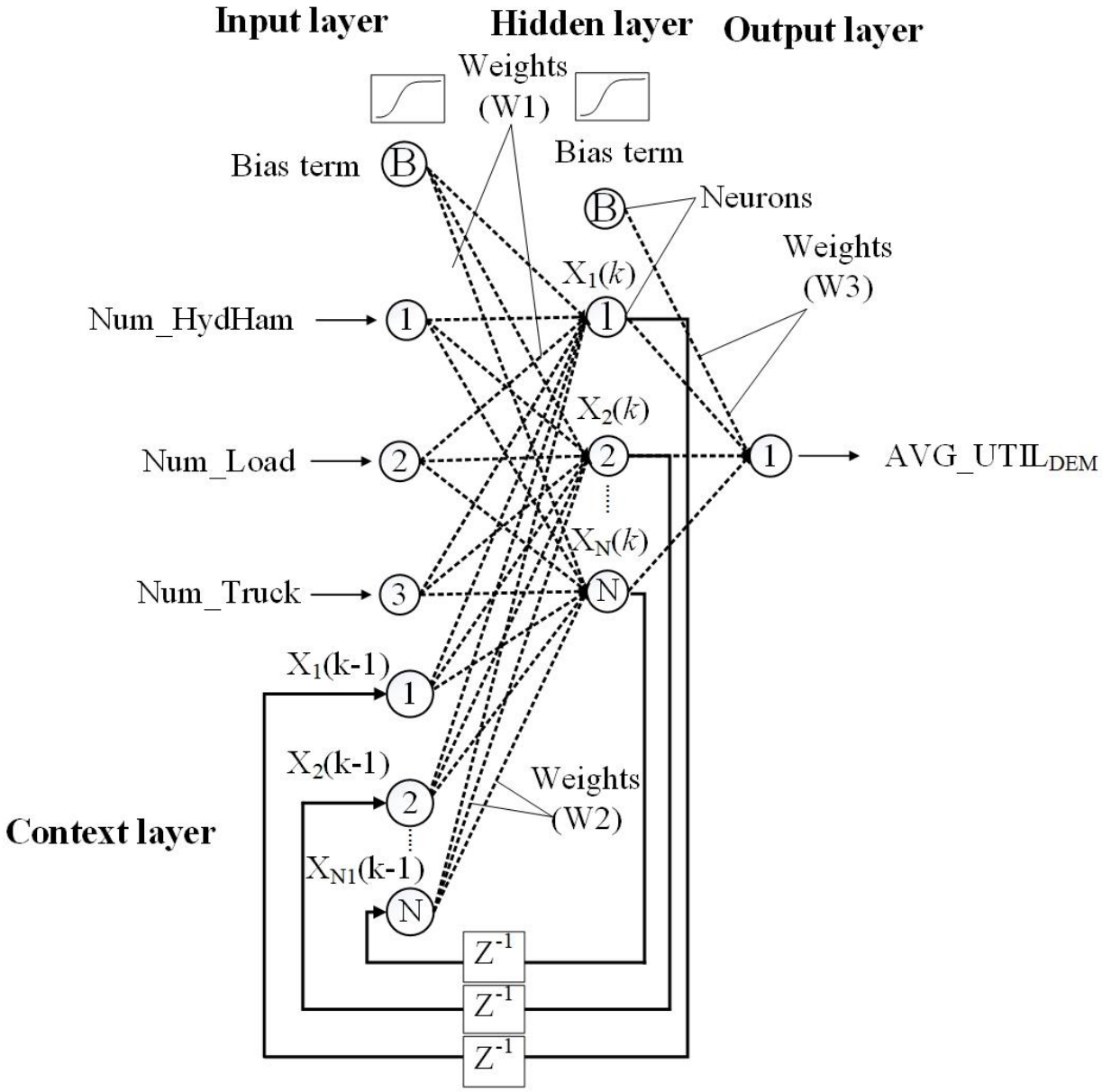
Input layer
Hidden layer
Output layer
Weights
(W1)
Bias term
Bias term
Neurons
Weights
(W3)
$X_1(k)$
Num_HydHam
$X_2(k)$
Num_Load
AVG_UTIL_{DEM}
$X_N(k)$
Num_Truck
$X_1(k-1)$
$X_2(k-1)$
Weights
(W2)
Context layer
$X_{N1}(k-1)$
Z^{-1}
Z^{-1}
Z^{-1}

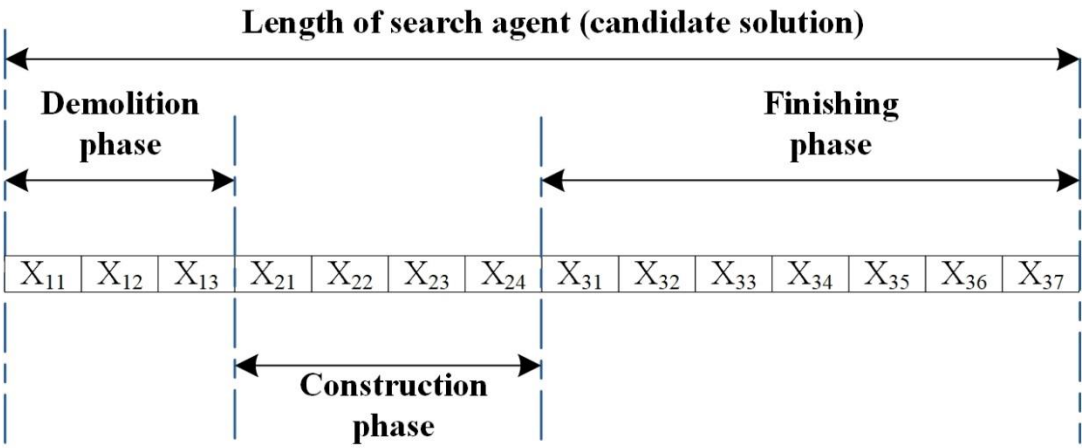

X_{ij}: Number of utilized resources of type *i* in phase *j* {1, 2, 3}

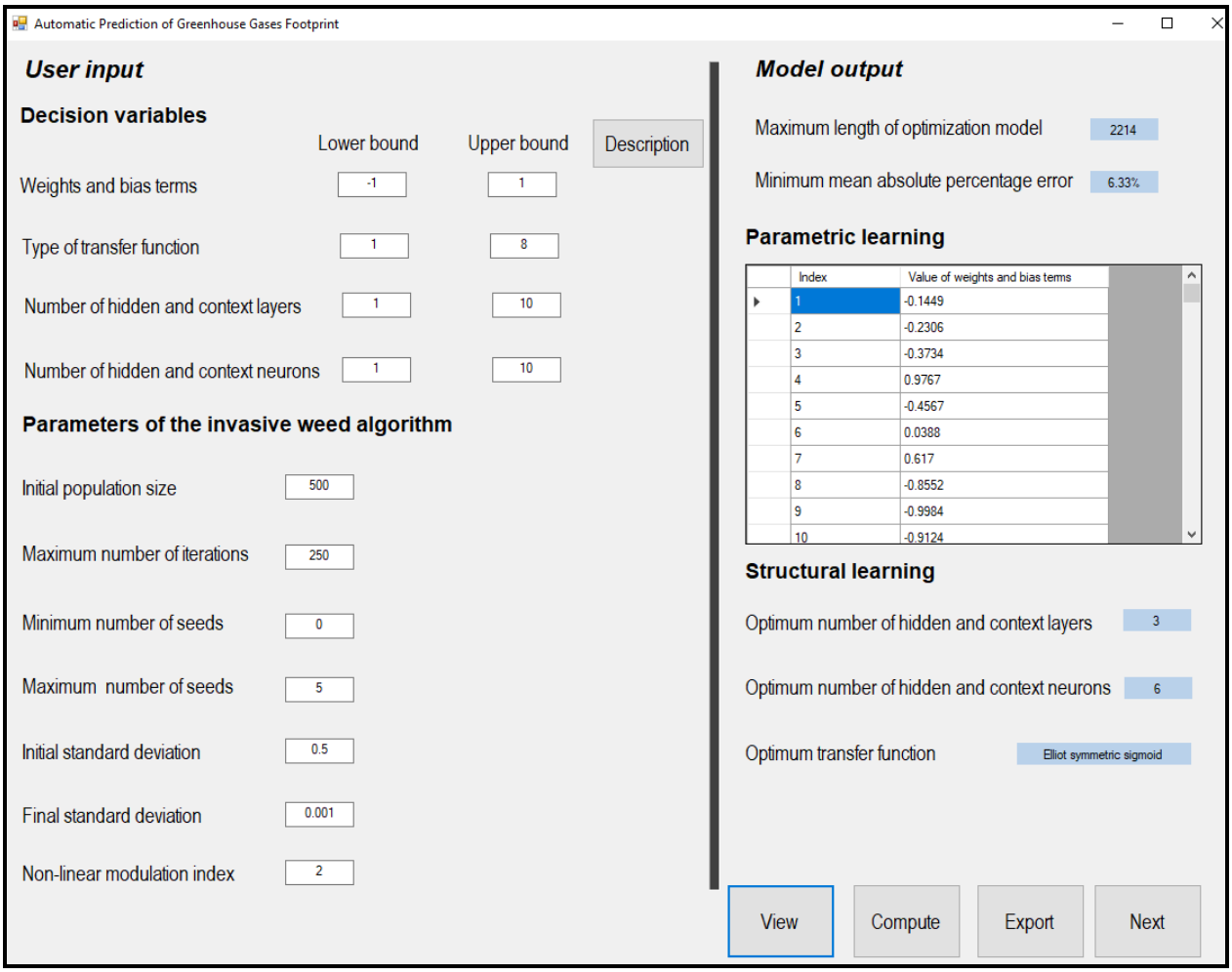
Automatic Prediction of Greenhouse Gases Footprint
User input
Decision variables
Lower bound
Upper bound
Description
Weights and bias terms
-1
1
Type of transfer function
1
8
Number of hidden and context layers
1
10
Number of hidden and context neurons
1
10
Parameters of the invasive weed algorithm
Initial population size
500
Maximum number of iterations
250
Minimum number of seeds
0
Maximum number of seeds
5
Initial standard deviation
0.5
Final standard deviation
0.001
Non-linear modulation index
2
Model output
Maximum length of optimization model
2214
Minimum mean absolute percentage error
6.33%
Parametric learning
Index
Value of weights and bias terms
1 -0.1449
2 -0.2306
3 -0.3734
4 0.9767
5 -0.4567
6 0.0388
7 0.617
8 -0.8552
9 -0.9984
10 -0.9124
Structural learning
Optimum number of hidden and context layers
3
Optimum number of hidden and context neurons
6
Optimum transfer function
Elliot symmetric sigmoid
View
Compute
Export
Next

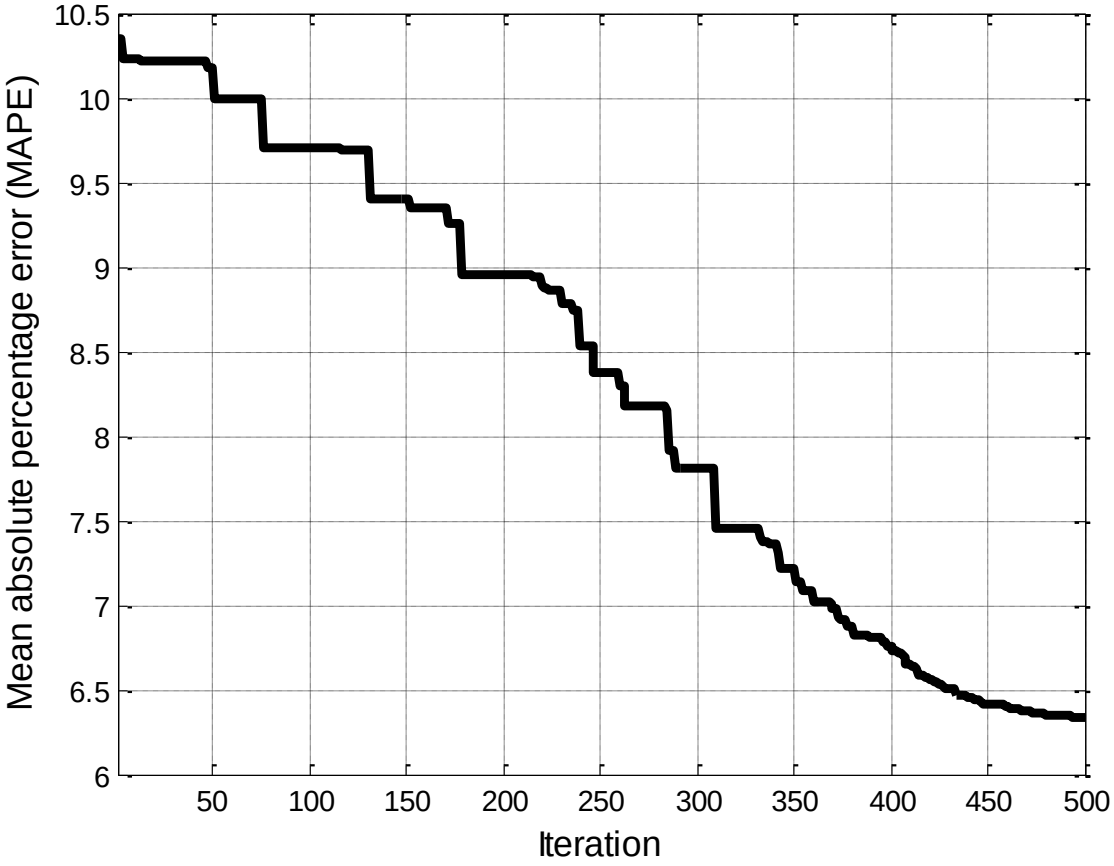
Mean absolute percentage error (MAPE)
10.5
10
9.5
9
8.5
8
7.5
7
6.5
6
50
100
150
200
250
300
350
400
450
500
Iteration

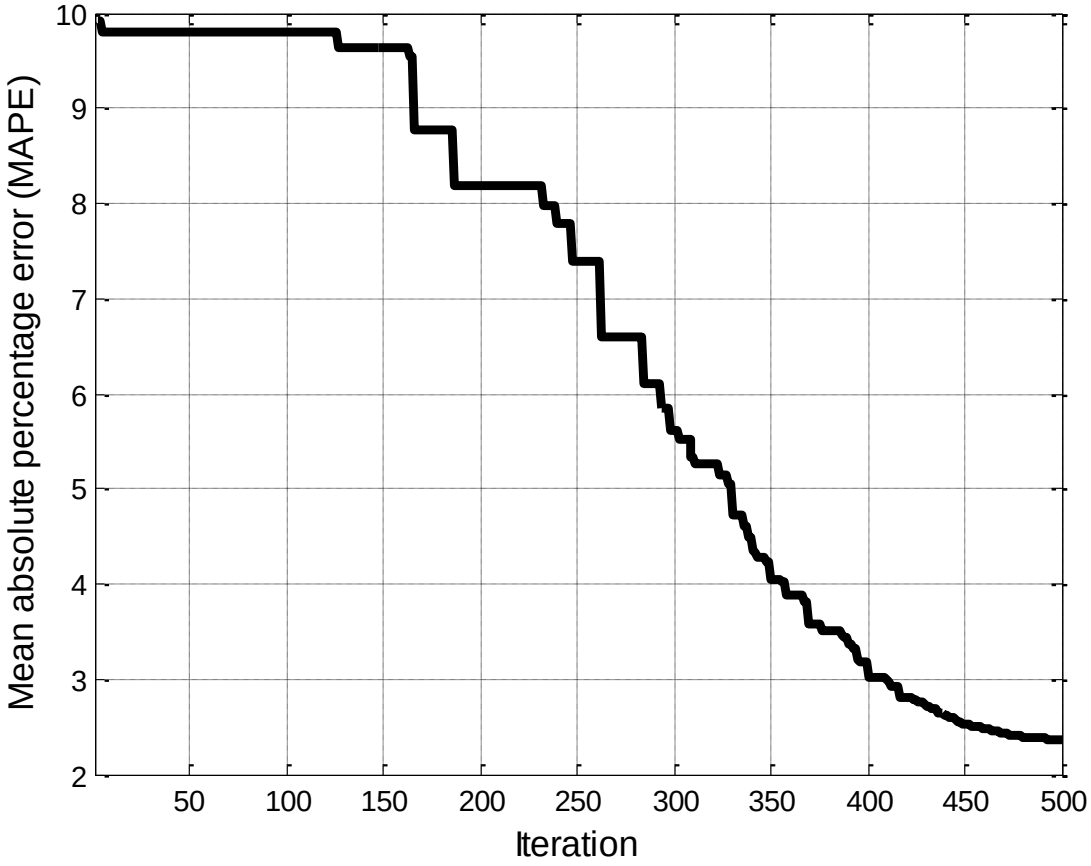
Mean absolute percentage error (MAPE)
10
9
8
7
6
5
4
3
2
50
100
150
200
250
300
350
400
450
500
Iteration

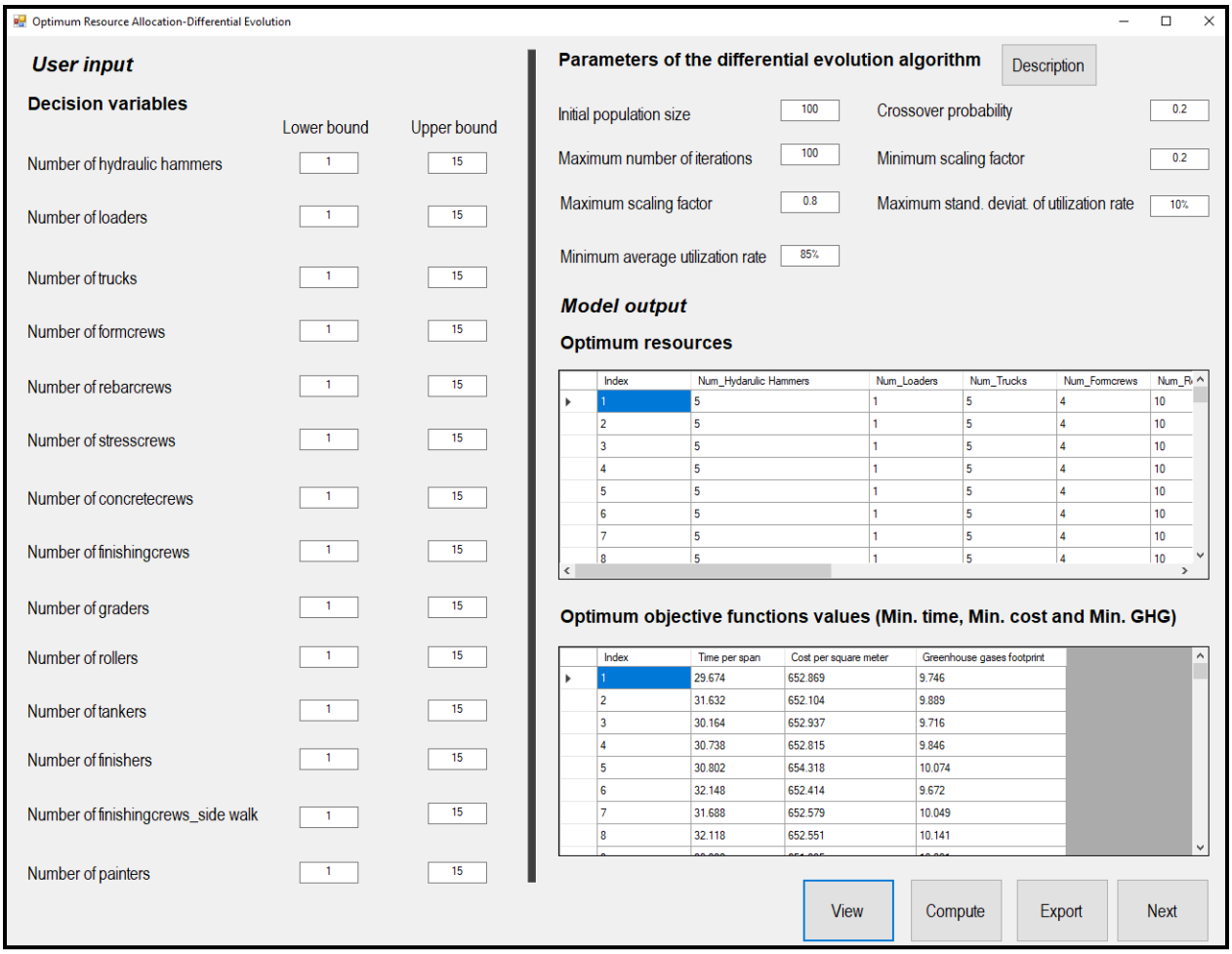
Optimum Resource Allocation-Differential Evolution
User input
Decision variables
Lower bound
Upper bound
Number of hydraulic hammers
1
15
Number of loaders
1
15
Number of trucks
1
15
Number of formcrews
1
15
Number of rebarcrews
1
15
Number of stresscrews
1
15
Number of concretecrews
1
15
Number of finishingcrews
1
15
Number of graders
1
15
Number of rollers
1
15
Number of tankers
1
15
Number of finishers
1
15
Number of finishingcrews_side walk
1
15
Number of painters
1
15
Parameters of the differential evolution algorithm
Description
Initial population size
100
Crossover probability
0.2
Maximum number of iterations
100
Minimum scaling factor
0.2
Maximum scaling factor
0.8
Maximum stand. deviat. of utilization rate
10%
Minimum average utilization rate
85%
Model output
Optimum resources
Index
Num_Hydarulic Hammers
Num_Loaders
Num_Trucks
Num_Formcrews
1 5 1 5 4 10
2 5 1 5 4 10
3 5 1 5 4 10
4 5 1 5 4 10
5 5 1 5 4 10
6 5 1 5 4 10
7 5 1 5 4 10
8 5 1 5 4 10
Optimum objective functions values (Min. time, Min. cost and Min. GHG)
Index
Time per span
Cost per square meter
Greenhouse gases footprint
1 29.674 652.869 9.746
2 31.632 652.104 9.889
3 30.164 652.937 9.716
4 30.738 652.815 9.846
5 30.802 654.318 10.074
6 32.148 652.414 9.672
7 31.688 652.579 10.049
8 32.118 652.551 10.141
View
Compute
Export
Next

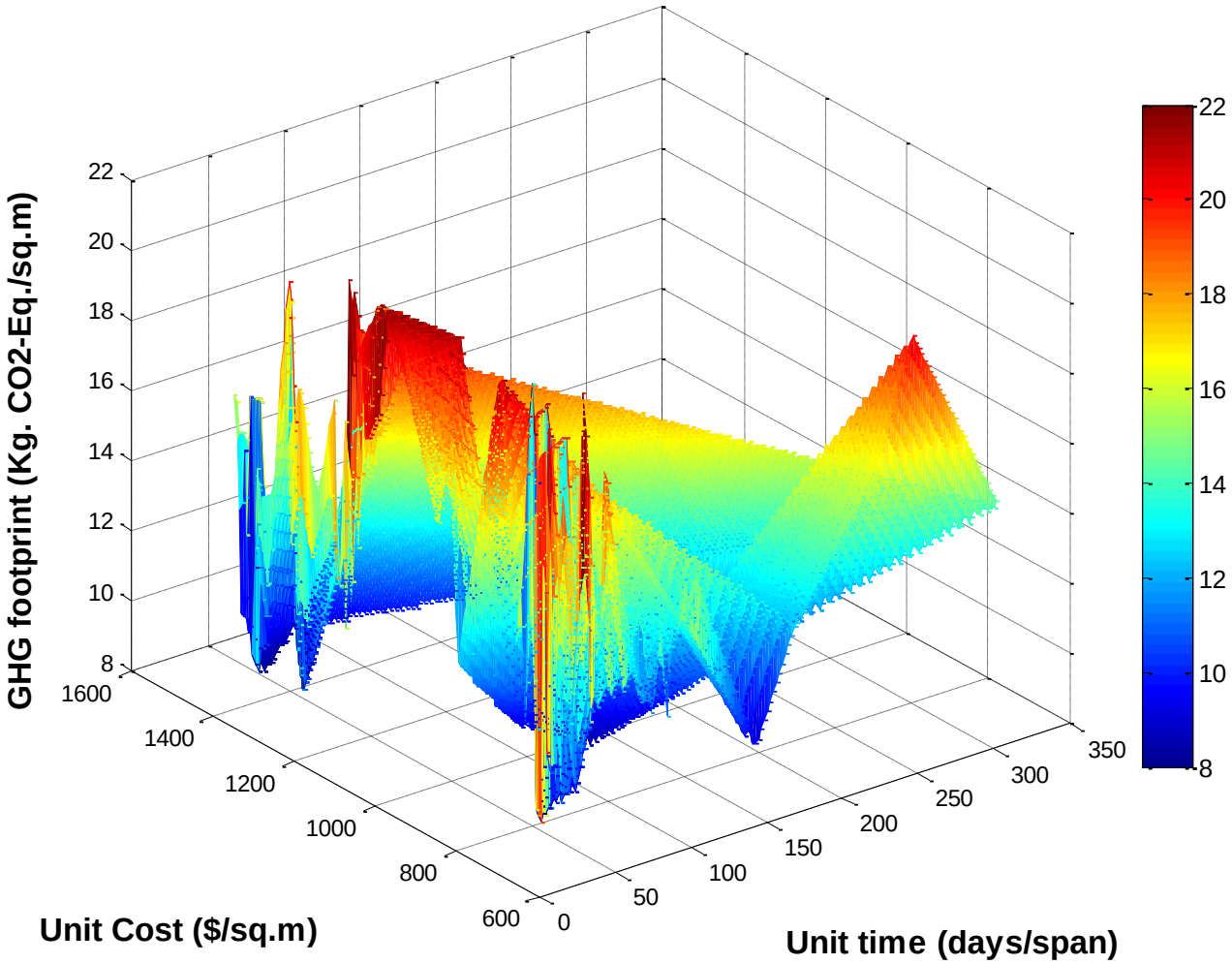
GHG footprint (Kg. CO2-Eq./sq.m)
22
20
18
16
14
12
10
8
1600
1400
1200
1000
800
600
Unit Cost ($/sq.m)
0
50
100
150
200
250
300
350
Unit time (days/span)
22
20
18
16
14
12
10
8

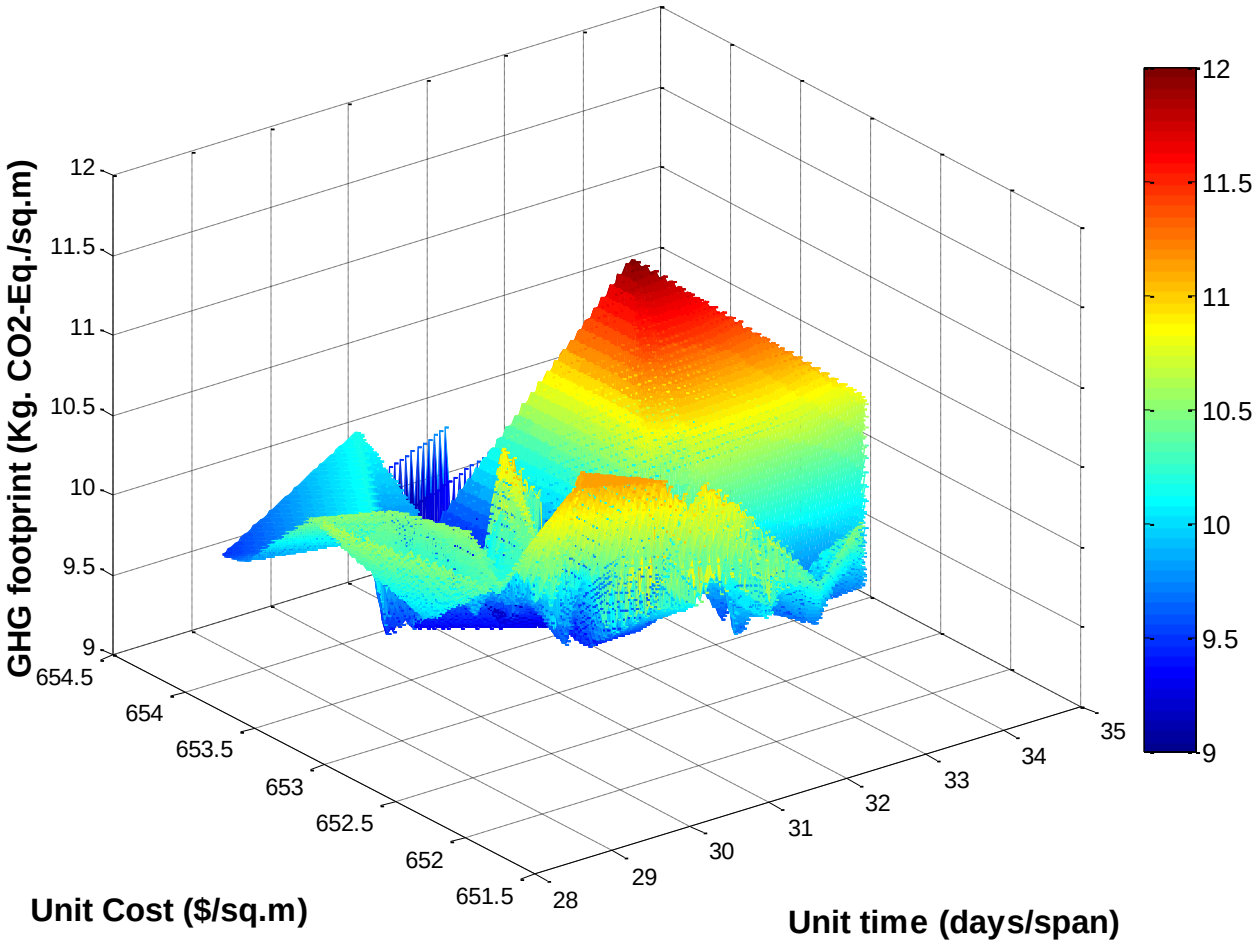
GHG footprint (Kg. CO2-Eq./sq.m)
12
11.5
11
10.5
10
9.5
9
654.5
654
653.5
653
652.5
652
651.5
Unit Cost ($/sq.m)
28
29
30
31
32
33
34
35
Unit time (days/span)
12
11.5
11
10.5
10
9.5
9

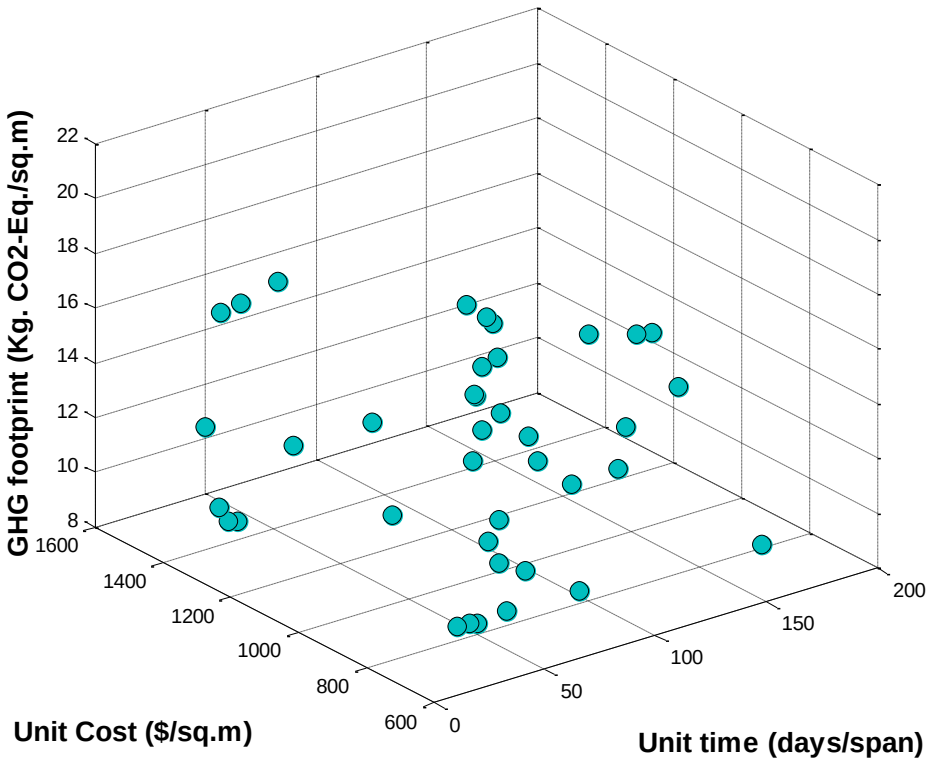

(a) Pareto optimal solutions computed from the multi-objective particle swarm optimization model

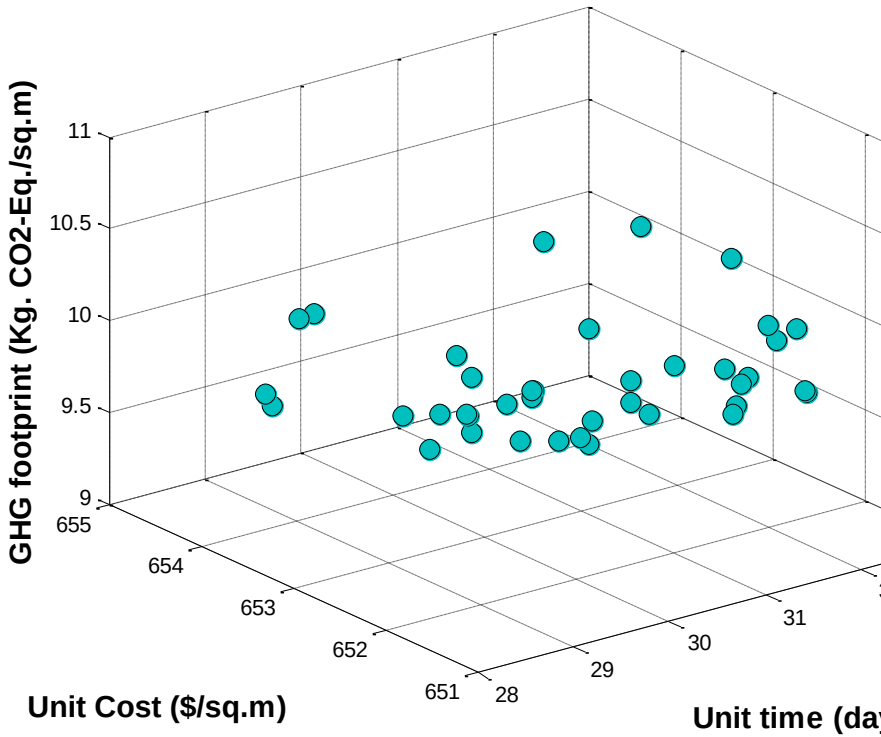

(b) Pareto optimal solutions computed from the multi-objective differential evolution model

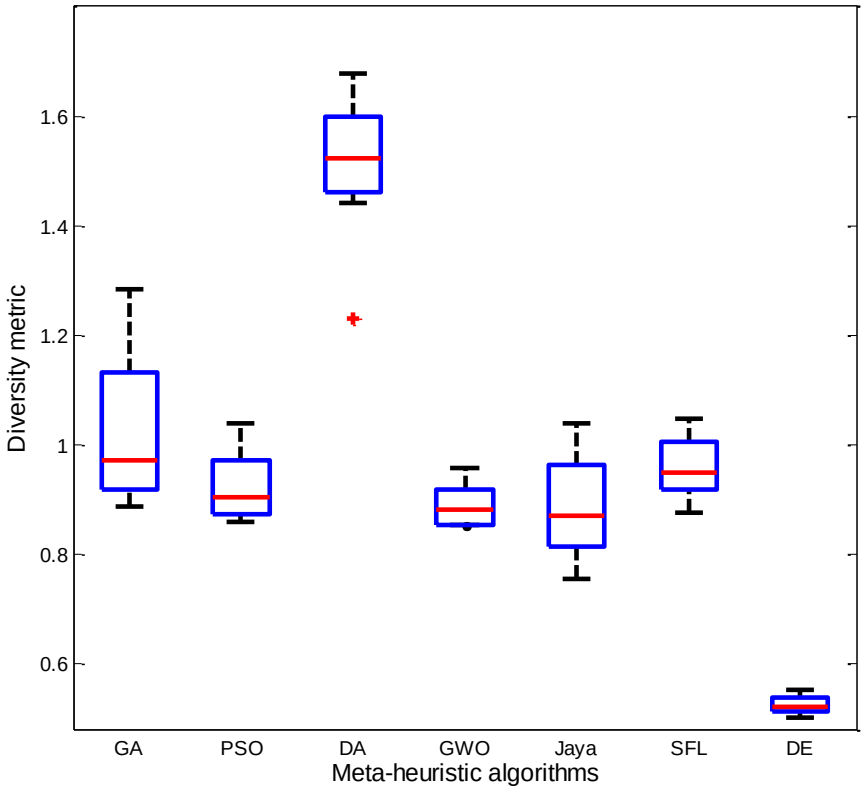

(a) Box plots of the diversity metric

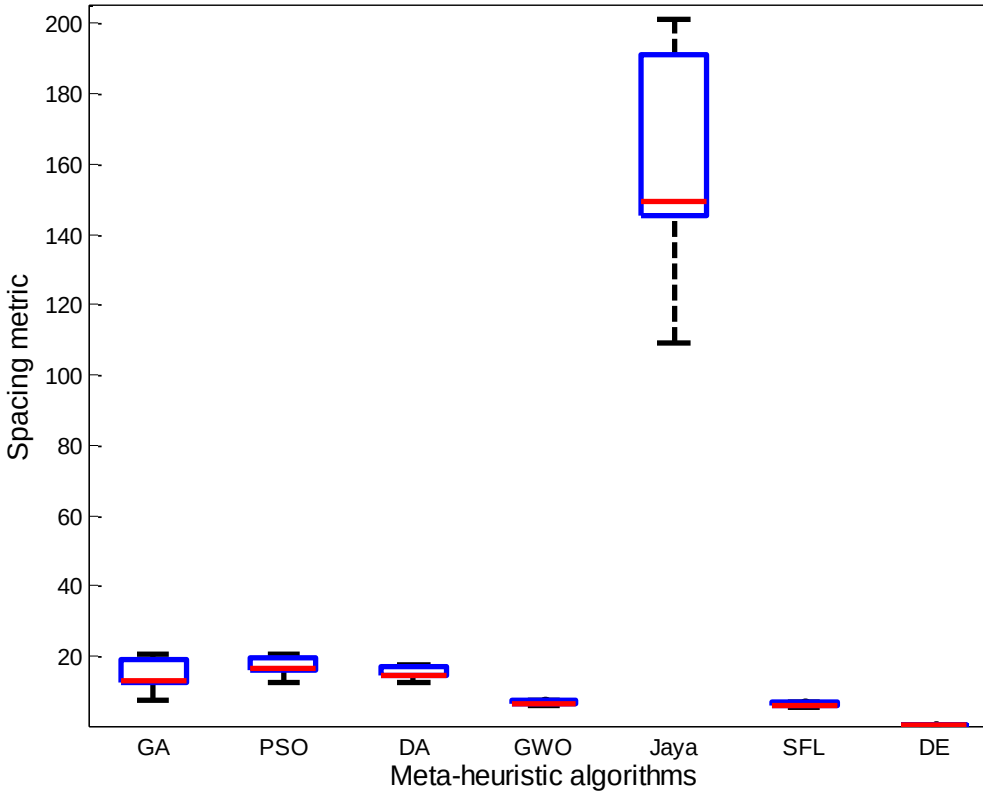

(b) Box plots of the generational distance

List of Tables

Table 1: STROBOSCOPE Simulation Elements

Simulation Element Name	Description
Queue	Queues hold resources that are idle to be utilized by the Combi activities. Each Queue is associated with a particular resource type
Combi	Combi activities represent activities that start when certain conditions are satisfied (the required resources are available in the preceding queue). In case it doesn't have a condition, it will be similar to Normal activity.
Normal	Normal activities represent activities that start immediately after other activities have ended. A Normal activity acquires the resources from the activity that has just finished.
Link	Links connect the network nodes and indicates the type and direction of resources flowing between the nodes
Consolidator	Consolidators represent a condition to release or hold the resources flow

Table 2: Input and output of the developed multi-objective optimization model

Input	Output
Parameters of differential evolution algorithm	Minimum time per span
Threshold of minimum average utilization rate	Minimum unit cost
Threshold of maximum standard deviation of utilization rate	Minimum greenhouse gases footprint
Lower and upper bound of decision variables	Optimum number of hydraulic hammers
Productivity rates of the crews	Optimum number of loaders
Hourly fuel consumption rates	Optimum number of trucks
Daily direct cost of the resource	Optimum number of form crews
Carbon emission factor	Optimum number of rebar crews
Density of diesel	Optimum number of stress crews
	Optimum number of concrete crews
	Optimum number of finishing crews
	Optimum number of graders
	Optimum number of rollers
	Optimum number of tankers
	Optimum number of finishers
	Optimum number of sidewalk finishing crews
	Optimum number of painting crews
	Optimum number of hydraulic hammers

Table 3: Boundary condition of the output variables from discrete event simulation model

Output variable	Boundary conditions
Time per span ($\mathbf{T_S}$,days/span)	4.572-50.909
Cost per square meter ($\mathbf{C_m}$,$/square meter)	344.351-794.027
Greenhouse gases per square meter ($\mathbf{GHG_m}$,Kg CO_2-Eq./square meter)	11.214-24.047
Average utilization rate of demolition phase ($\mathbf{AVG\_UTIL_{DEM}}$, %)	72.931-99.989
Standard deviation of utilization rate of demolition phase ($\mathbf{STD\_UTIL_{DEM}}$, %)	2.01-38.142
Average utilization rate of construction phase ($\mathbf{AVG\_UTIL_{CONST}}$, %)	60.451-90.141
Standard deviation of utilization rate of construction phase ($\mathbf{STD\_UTIL_{CONST}}$, %)	10.408-43.543
Average utilization rate of finishing phase ($\mathbf{AVG\_UTIL_{FINISH}}$, %)	84.91-99.958
Standard deviation of utilization rate of finishing phase ($\mathbf{STD\_UTIL_{FINISH}}$, %)	3.018-12.365

Table 4: P − values of the simulation and machine learning models using Shapiro-Wilk test for normality

Model	Description	P − value
T_S	Discrete event simulation	0 (H_1)
T_S	Machine learning	0 (H_1)
C_m	Discrete event simulation	0 (H_1)
C_m	Machine learning	0 (H_1)
GHG_m	Discrete event simulation	1.54×10^{-3} (H_1)
GHG_m	Machine learning	0 (H_1)
AVG_UTIL_{DEM}	Discrete event simulation	0 (H_1)
AVG_UTIL_{DEM}	Machine learning	0 (H_1)
STD_UTIL_{DEM}	Discrete event simulation	0 (H_1)
STD_UTIL_{DEM}	Machine learning	0 (H_1)
AVG_UTIL_{CONST}	Discrete event simulation	0 (H_1)
AVG_UTIL_{CONST}	Machine learning	0 (H_1)
STD_UTIL_{CONST}	Discrete event simulation	0 (H_1)
STD_UTIL_{CONST}	Machine learning	0 (H_1)
AVG_UTIL_{FINISH}	Discrete event simulation	0 (H_1)
AVG_UTIL_{FINISH}	Machine learning	0 (H_1)
STD_UTIL_{FINISH}	Discrete event simulation	0 (H_1)
STD_UTIL_{FINISH}	Machine learning	0 (H_1)

Table 5: Statistical comparison between the different discrete event simulation and machine learning models based on Mann-Whitney-U test

Model	P – value
T_S	8.31×10^{-1} (H_0)
C_m	5.41×10^{-1} (H_0)
GHG_m	9.09×10^{-1} (H_0)
AVG_UTIL_{DEM}	1.6×10^{-1} (H_0)
STD_UTIL_{DEM}	6.09×10^{-1} (H_0)
AVG_UTIL_{CONST}	1.45×10^{-1} (H_0)
STD_UTIL_{CONST}	8.43×10^{-1} (H_0)
AVG_UTIL_{FINISH}	5.89×10^{-2} (H_0)
STD_UTIL_{FINISH}	3.11×10^{-1} (H_0)

Table 6: Performance comparison between the different machine learning models for the prediction of cost based on split validation

Type of machine learning model	Mean absolute percentage error (MAPE)	Mean absolute error (MAE)	Root-mean squared error (RMSE)
$\mathrm{ENN}-\mathrm{IWO}$	4.873%	78.466	39.515
ANN	8.290%	78.927	49.097
RBNN	8.003%	129.842	61.409
GRNN	8.278%	89.205	51.976
CNN	7.839%	80.102	63.901
LSVM	18.361%	214.525	111.639
RSVM	17.990%	212.867	110.144
GBDT	8.134%	81.006	60.037
GP	20.223%	269.505	173.650
$\mathrm{K}-\mathrm{NN}$	7.903%	86.572	51.242

Table 7: Performance comparison between the different machine learning models for the prediction of greenhouse gases based on split validation

Type of machine learning model	Mean absolute percentage error (MAPE)	Mean absolute error (MAE)	Root-mean squared error (RMSE)
$\mathrm{ENN}-\mathrm{IWO}$	6.67%	1.53	1.163
ANN	12.001%	2.844	1.948
RBNN	11.725%	3.055	2.038
GRNN	10.939%	3.006	2.127
CNN	8.753%	1.772	1.436
LSVM	9.104%	1.869	1.490
RSVM	8.406%	1.949	1.293
GBDT	8.277%	1.638	1.346
GP	24.879%	5.713	4.117
$\mathrm{K}-\mathrm{NN}$	8.118%	1.672	1.333

Table 8: Performance comparison between the different machine learning models for the prediction of greenhouse gases based on 10-fold cross validation

Type of machine learning model	Mean absolute percentage error	Mean absolute error	Root-mean squared error
$\mathrm{ENN}-\mathrm{IWO}$	7.417%	1.701	1.293
ANN	13.501%	3.202	2.191
RBNN	13.132%	3.425	2.283
GRNN	12.284%	3.385	2.391
CNN	9.813%	1.988	1.612
LSVM	10.218%	2.105	1.681
RSVM	9.457%	2.196	1.458
GBDT	9.302%	1.841	1.514
GP	28.113%	6.473	4.669
$\mathrm{K}-\mathrm{NN}$	9.096%	1.874	1.497

Table 9: Statistical comparison for the developed cost prediction model against other models based on non-parametric tests

Pair of prediction models	Wilcoxn	Mann-Whitney-U	Kruskal–Wallis	Binomial sign
ENN − IWO, ANN	H_1 (P − value $=4.48\times10^{-3}$)	H_1 (P − value $=1.83\times10^{-4}$)	H_1 (P − value =0)	H_1 (P − value =0)
ENN − IWO, RBNN	H_1 (P − value $=3.87\times10^{-3}$)	H_1 (P − value $=1.83\times10^{-4}$)	H_1 (P − value =0)	H_1 (P − value =0)
ENN − IWO, GRNN	H_1 (P − value $=4.81\times10^{-3}$)	H_1 (P − value $=1.83\times10^{-4}$)	H_1 (P − value =0)	H_1 (P − value =0)
ENN − IWO, CNN	H_1 (P − value $=4.07\times10^{-3}$)	H_1 (P − value $=4.4\times10^{-4}$)	H_1 (P − value =0)	H_1 (P − value =0)
ENN − IWO, LSVM	H_1 (P − value $=1.57\times10^{-3}$)	H_1 (P − value $=1.83\times10^{-4}$)	H_1 (P − value =0)	H_1 (P − value =0)
ENN − IWO, RSVM	H_1 (P − value $=4.25\times10^{-3}$)	H_1 (P − value $=1.83\times10^{-4}$)	H_1 (P − value =0)	H_1 (P − value =0)
ENN − IWO, GBDT	H_1 (P − value $=4.4\times10^{-3}$)	H_1 (P − value $=1.83\times10^{-4}$)	H_1 (P − value =0)	H_1 (P − value =0)
ENN − IWO, GP	H_1 (P − value $=4.38\times10^{-3}$)	H_1 (P − value $=1.83\times10^{-4}$)	H_1 (P − value =0)	H_1 (P − value =0)
ENN − IWO, K − NN	H_1 (P − value $=4.48\times10^{-3}$)	H_1 (P − value $=1.83\times10^{-4}$)	H_1 (P − value =0)	H_1 (P − value =0)

Table 10: Statistical comparison for the developed greenhouse gases prediction model against other models based on non-parametric tests

Pair of prediction models	Wilcoxn	Mann-Whitney-U	Kruskal–Wallis	Binomial sign
ENN − IWO, ANN	H_1 (P − value =4.38×10^{-3})	H_1 (P − value =1.83×10^{-4})	H_1 (P − value =0)	H_1 (P − value =0)
ENN − IWO, RBNN	H_1 (P − value =4.4×10^{-3})	H_1 (P − value =1.83×10^{-4})	H_1 (P − value =0)	H_1 (P − value =0)
ENN − IWO, GRNN	H_1 (P − value =4.51×10^{-3})	H_1 (P − value =1.83×10^{-4})	H_1 (P − value =0)	H_1 (P − value =0)
ENN − IWO, CNN	H_1 (P − value =3.87×10^{-3})	H_1 (P − value =2.2×10^{-4})	H_1 (P − value =2×10^{-3})	H_1 (P − value =0)
ENN − IWO, LSVM	H_1 (P − value =3.51×10^{-3})	H_1 (P − value =1.83×10^{-3})	H_1 (P − value =1×10^{-3})	H_1 (P − value =0)
ENN − IWO, RSVM	H_1 (P − value =3.58×10^{-3})	H_1 (P − value =7.69×10^{-4})	H_1 (P − value =7×10^{-3})	H_1 (P − value =0)
ENN − IWO, GBDT	H_1 (P − value =3.87×10^{-3})	H_1 (P − value =7.28×10^{-3})	H_1 (P − value =7×10^{-3})	H_1 (P − value =0)
ENN − IWO, GP	H_1 (P − value =4.09×10^{-3})	H_1 (P − value =1.83×10^{-4})	H_1 (P − value =0)	H_1 (P − value =0)
ENN − IWO, K − NN	H_1 (P − value =4.02×10^{-3})	H_1 (P − value =1.13×10^{-2})	H_1 (P − value =1×10^{-2})	H_1 (P − value =0)

Table 11: Performance comparison between the different multi-objective optimization algorithms

Performance metric	Objective function	NLP	MOGA	MOPSO	MODA	MOGWO	MOJAYA	MOSFL	MODE
Average	T_S	59.026	105.382	54.634	31.916	32.636	48.102	46.108	**30.549**
	C_m	1444.287	904.842	907.965	771.511	1014.708	852.132	682.99	**652.629**
	GHG_m	19.549	16.447	15.515	17.017	13.426	16.946	13.606	**9.984**
Coefficient of variation	T_S	…….	61.849 %	90.980 %	30.275 %	4.035 %	176.729%	18.555 %	**5.760 %**
	C_m	…….	29.164 %	32.983 %	31.611 %	27.095 %	24.671 %	7.369 %	**0.084 %**
	GHG_m	…….	23.222 %	26.844 %	21.747 %	12.587 %	22.488 %	22.516 %	**3.794 %**
Hypervolume indicator	…….	…….	47.341 %	23.140 %	20.112 %	22.586 %	28.374 %	74.265 %	**81.721 %**
Generational distance	…….	…….	0.9563	2.2969	0.0489	0.3003	5.482	3.1475	**0.029**
Spacing	…….	…….	14.2611	16.939	14.9645	6.6787	157.4636	6.0265	**0.1881**
Diversity	…….	…….	1.0138	0.9163	1.5165	0.8874	0.8855	0.9587	**0.5229**
Spread	…….	…….	0.6047	0.4394	0.5152	0.7329	0.7832	0.7353	**0.9618**
Coverage	…….	…….	0.955	0.7505	0.9249	0.9997	0.9488	0.8006	**0.4087**

Table 12: Statistical comparison between the different multi-objective optimization models as per hypervolume indicator using non-parametric testing

Pair of optimization models	Wilcoxn	Mann-Whitney-U	Kruskal–Wallis	Binomial sign
MODE, MOGA	H_1 (P – value $=5.12\times10^{-3}$)	H_1 (P – value $=2\times10^{-4}$)	H_1 (P – value =0)	H_1 (P – value =0)
MODE, MOPSO	H_1 (P – value $=5.12\times10^{-3}$)	H_1 (P – value $=2\times10^{-4}$)	H_1 (P – value =0)	H_1 (P – value =0)
MODE, MODA	H_1 (P – value $=5.12\times10^{-3}$)	H_1 (P – value $=2\times10^{-4}$)	H_1 (P – value =0)	H_1 (P – value =0)
MODE, MOGWO	H_1 (P – value $=5.12\times10^{-3}$)	H_1 (P – value $=2\times10^{-4}$)	H_1 (P – value =0)	H_1 (P – value =0)
MODE, MOJAYA	H_1 (P – value $=5.12\times10^{-3}$)	H_1 (P – value $=2\times10^{-4}$)	H_1 (P – value =0)	H_1 (P – value =0)
MODE, MOSFL	H_1 (P – value $=5.12\times10^{-3}$)	H_1 (P – value $=2\times10^{-4}$)	H_1 (P – value =0)	H_1 (P – value =0)

Table 13: Entropy values, variation coefficients, and the weights of the attributes

Index	T_S	C_m	GHG_m
Entropy value (e_j)	5.7502	5.7706	5.7691
variation coefficient (d_j)	0.00895	0.00544	0.00568
weights of the attribute (w_j)	44.588%	27.102%	28.31%

Table 14: Sample of the solutions' rankings obtained from PROMETHEE II

Optimum solution	Optimum objective function values	Meta-heuristic	Net flow ($\phi(a)$)	Ranking
[5, 1, 5, 4, 10, 7, 10, 5, 5, 8, 10, 6, 5, 1]	[29.742, 652.918, 9.719]	MODE	0.2213	1
[5, 1, 5, 4, 10, 7, 10, 4, 5, 10, 10, 6, 5, 1]	[30.304, 652.817, 9.762]	MODE	0.2165	8
[5, 2, 5, 4, 6, 7, 7, 1, 4, 9, 7, 4, 4, 5]	[30.469,652.567, 10.208]	MODE	0.2123	14
[5, 2, 1, 6, 7, 6, 6, 2, 4, 11, 6, 8, 4, 4]	[28.685, 1422.838, 12.731]	MODA	0.2078	29
[3, 4, 4, 5, 7, 5, 3, 5, 4, 12, 5, 7, 5, 2]	[40.896, 658.032, 10.781]	MOSFL	0.2066	32